THE MICROCIRCULATION: THEORY AND EXPERIMENT

Harvey N. Mayrovitz

A DISSERTATION

in

Bioengineering

Presented to the Faculty of the Graduate School of Arts and Sciences of the University of Pennsylvania in Partial Fulfillment of the Requirements for the Degree of Doctor of Philosophy.

1974

Abraham Noordergraaf
Supervisor of Dissertation

Lyle H. Peterson
Supervisor of Dissertation

Abraham Noordergraaf
Graduate Group Chairman

PART 3 - Chapter 5 SIMULATION RESULTS

CHAPTER FIVE... RESULTS OF MICROVASCULAR SIMULATION

I. Introduction

In this chapter, the results obtained from the computer simulation of the Microvascular Model are presented. These results are separated into two broad categories.

First, (Section II) the results obtained from the model without the complexities of parameter variation are presented. The model parameters corresponding to this state are thus time in variant, and, for simplicity, the model is referred to as the passive model. The simulation of this model state is achieved by inactivating the rhythmically active vessel (venomotion) and the terminal arteriole and precapillary sphincter (vasomotion) programs. Under these conditions, all parameters of the simulated vascular region are constant, and have values equal to their mean values.

Three aspects of the passive model are investigated, and where experimental data from the literature is available, the model results are compared. In Section II-A, the mean pressure distribution throughout the microvasculature predicted by the model, and compared with experimental data, is presented. In Section II-B, the passive model properties with respect to the transmission of pulsatile arterial pressure are investigated. Both attenuation and phase characteristics are evaluated and compared with experimental data.

Where the rhythmically active vessel and/or the precapillary sphincter programs are activated, the model and accompanying simulation are referred to as active. Thus, the second and principal

category of results (Section III) is for the active model.

In Section III-A, the hemodynamic effects of venomotion are studied by activating the venomotion program and examining the parameter variations, pressures, and flows in the vascular region bounded by the pressures P_5 and P_{10} as shown in figure 4.10.

The first objective (Section A.1) is to determine the relationship between the parameters of the model and effective wall stress.

The next objective is to separate and study the intrinsic hemodynamics associated with venomotion. Specifically, we seek an answer to the following three questions. What are the pressures and flows associated with rhythmically active microvessels in which hydraulic resistance and vessel compliance are uniformly varying throughout the vessel length? What effect does the presence of valves have on these hemodynamics? What effect does axially non-uniform parameter variation produce on these hemodynamics?

To answer these questions, results are obtained (Section A.2) for the simulated situation in which there is no imposed pressure gradient. Under these conditions, the dynamic pressures and flows are due to venomotion only.

In Section A.2(a), the results obtained for uniform contraction without the valves are presented, and in part (iiii) of that section, the results of inclusion of the valves are presented.

In Section A.2(b), the results obtained for the non-uniform contraction mode are presented and compared with the uniform case.

The next objective is to study the hemodynamics associated with venomotion under the physiological condition in which a non-zero imposed pressure gradient is present. These results are presented in Section A.3.

In Section III-B, the separate and combined effects of venomotion and vasomotion on capillary and pre capillary hemodynamics are studied by examining the pressures, flows, and filtration characteristics in the vascular region bounded by the pressures P_3 and P_5, as shown in figure 4.10.

To determine the effect of post capillary dynamics (venomotion) on capillary flow, results are obtained relating capillary flow to active venous dynamics in the absence (B.1) and presence (B.2) of pulsatile arterial pressure, but without the presence of arteriole vasomotion.

The general question of the hemodynamic effects of arteriole vasomotion is taken up in Section B.3, where results are obtained without the presence of venomotion. The first aspect studied (Section B.3a) is the characteristics of the arteriole diameter variation and associated hemodynamics. Next (in Section B.3b), the effects of these hemodynamics on capillary pressure, flow and filtration are studied.

In Section B.4, results illustrating the combined effect of vasomotion and venomotion on capillary hemodynamics are obtained and presented.

II. Passive Model Results

A. Pressure Distribution in the Passive Model

For reference purposes, the Microvascular Model, originally shown in figure 4.10, is here repeated. In Table 5.1 the parameter values used for the passive model simultaion in the example discussed below are listed. In the simulation the mean arterial pressure is adjusted from 66 mm Hg. This value approximates the mean value determined by Nicoll (1969). The resultant pressure distribution is then determined. The mean values of some of the quantities obtained from the simulation are shown in figure 4.10. The numerical values of pressure are all in mm Hg. All hemodynamic quantities so obtained were checked using numerical calculations. The results of the checking procedure showed the model to be computationally free of error. To assess the physiological accuracy of the model, a comparison was made between pertinent, but very limited, experimental data from the literature. It was found that the general characteristics of the pressure and flow distribution obtained from the model are consistent with experimental data obtained from mesentery and cremaster preparations (Zweifach, 1971; Intaglietta, 1970; Richardson and Zweifach, 1970).

Measurements made in the bat wing are quite limited. Mean small vein pressure has been measured to be 12 mm Hg (Wiederhielm, 1968) and 12 to 16 mm Hg (Nicoll, 1969). The value obtained from the model is 13.7 mm Hg, which is fully consistent with the experimental measurements. Direct measurements of the tissue colloid osmotic pressure

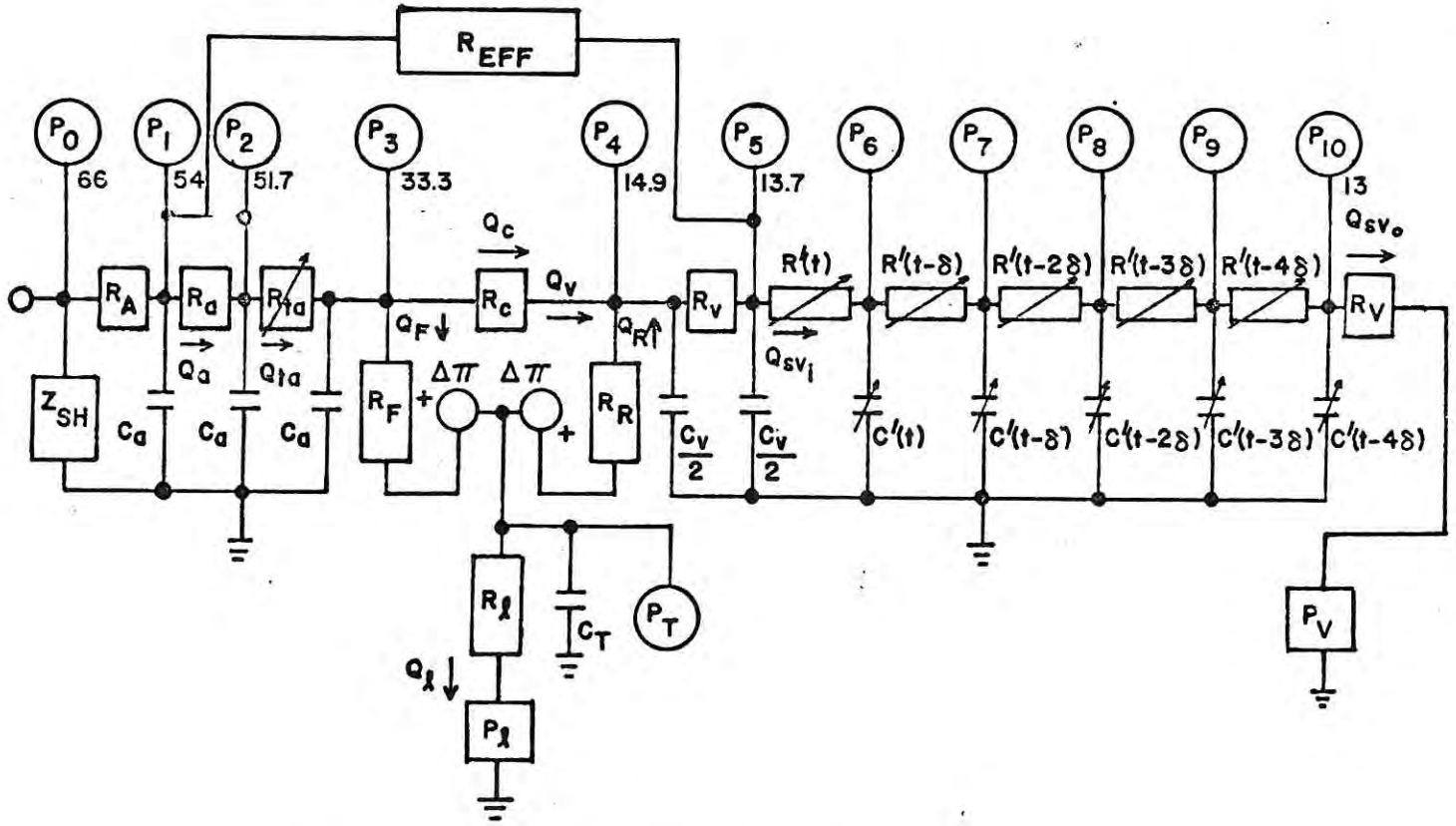

Figure 4.10. **DETAILED MICROVASCULAR MODEL**
Parameters defined in Table 4.3. Numbers adjacent to pressure symbols (circles) are the measured pressures at these points in mmHg.

Table 5.1 Parameter Values of Passive Model

Parameters correspond to those shown in figure 4.10 and defined in Chapter Four, Section A. Resistances are in units of dyne sec cm^{-5}, compliances in units of $dynes^{-1}$ cm^{5}, pressures in units of dynes cm^{-2}.

Symbol	Value
R_A	1.1×10^{10}
R_a	2.0×10^{10}
R_{ta}	1.6×10^{11}
R_c	1.6×10^{11}
R_F	3.2×10^{11}
R_R	3.2×10^{11}
R_l	3.2×10^{12}
R_v	8.8×10^{9}
$R'(t)$	5.0×10^{8}
R_V	1.0×10^{10}
C_a	1.0×10^{-13}
C_v	2.8×10^{-11}
$C'(t)$	7.0×10^{-12}
C_T	5.4×10^{-12}
$\Delta\pi$	2.0×10^{4}
P_l	3.0×10^{3}

in the wing have not been made. From measurements in other tissues, however (Källskog, 1973), the osmotic pressure difference that is measured under normal conditions is about 21 mm Hg. Using this value the model predicts a mean tissue pressure of 2.9 mm Hg. Measured values of tissue pressure using small hypodermic needles or micropipettes (Burch and Sodeman, 1937; Wells et al., 1938; Wiederheilm, 1969) have ranged from 1 to 5 mm Hg. The values predicted by the model are thus consistent with these experimental data.

No values of filtration or lymph flow have been reported for the bat wing. Data from the rat cremaster (Smaje et al., 1970) would indicate a filtration coefficient of the order of .001 cubic microns per second per square micron of capillary surface per cm. water pressure difference. Calculating the surface area of a single capillary pathway in the wing shows that the filtration flow should be a small fraction of the capillary net flow providing a similar value of filtration coefficient is applicable. The measurements of the capillary flow in the model with respect to exchange flow show this relationship to hold for the model. Thus, the various physiological properties of the composite model are consistent with available experimental data and show no significant variations which run counter to experimental evidence.

B. Pressure Transmission Characteristics

Figure 5.1 illustrates the attenuation and phase characteristics of the Microvascular Model. The attenuation of the simulated arterial pulsatile pressure, due to the microvasculature, is shown by

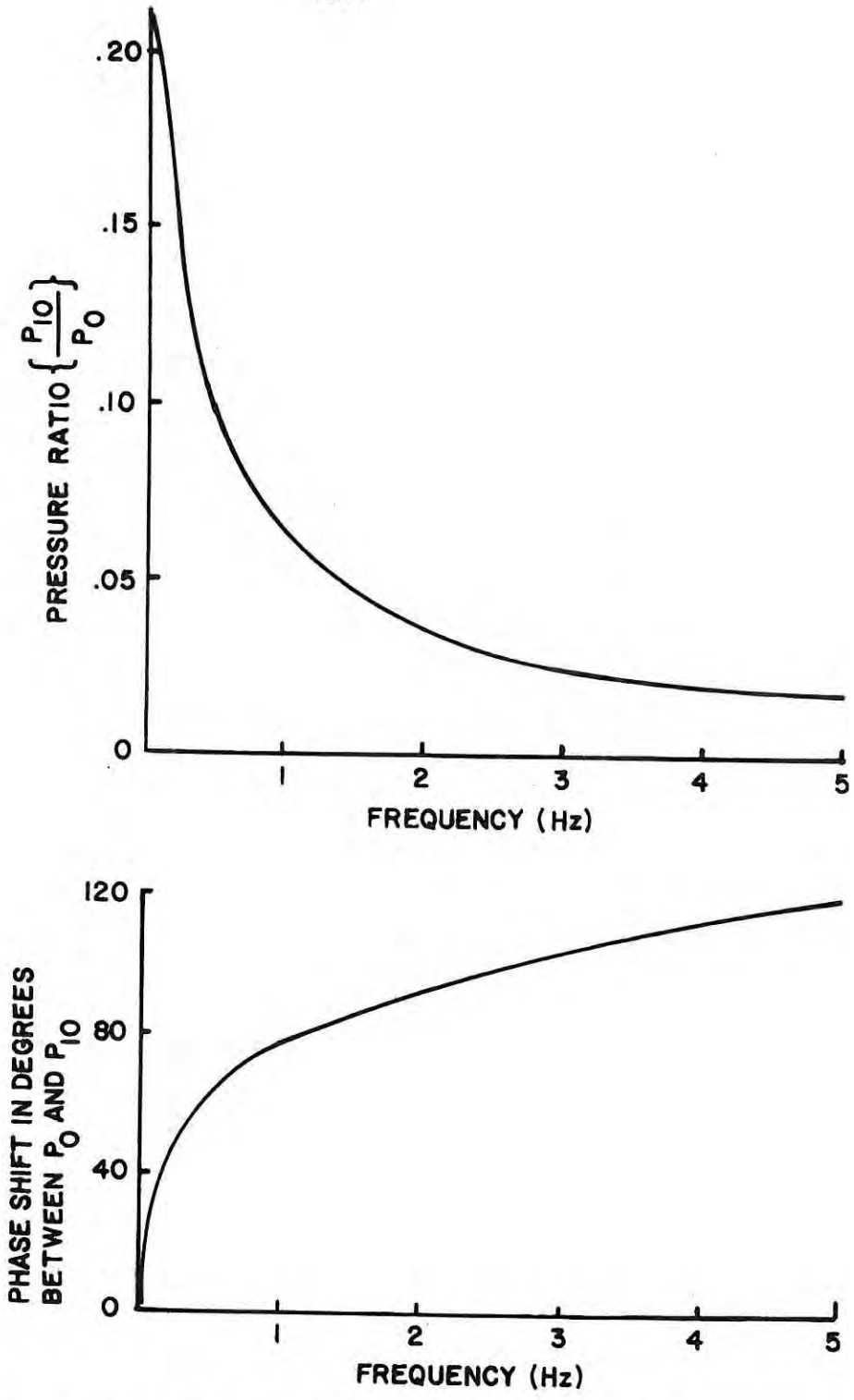

Figure 5.1. Attenuation and phase characteristics of the microvascular model. Pressure attenuation shown as the ratio of instantaneous venous pressure (P_{10} of Model) to arterial pressure (P_0). Phase characteristics shown as phase shift in degrees between these same pressures.

plotting the ratio of the peak to peak venous pressure (P_{10} of the model) to P_0. The phase characteristic is shown as a phase shift in degrees between these same two pressures. The only available experimental data in the literature with which the present results may be compared are for those obtained in the cat omentum (Intaglietta et al., 1971). Phase shift of the pressure fundamental frequency (2.5 Hz) and pressure attenuation was measured throughout the microvasculature. The phase shift they recorded from arterial vessels to venous vessels (diameter 40 microns) corresponds roughly to the microvasculature for which the presents results are applicable. They measured a phase shift of about 100 degrees through this microvasculature region and a pressure transmission ratio (equivalent to P_{10}/P_0) of .05. The Model prediction at a fundamental frequency of 2.5 Hz (the experimental case) is 98 degrees, and the transmission ratio is .03. Thus, it appears that the simulation results compare quite closely to the experimental results with respect to phase shift, but predict more attenuation of the arterial pulse. This difference in attenuation of pressure may be due to the fact that in the mesentery so called preferential channels which do not pass through the true capillaries are present. Such a topology would be expected to attenuate the arterial pulse less than a vascular bed in which no such channels are present, as is the case in the bat wing.

III. Active Model Results

A. Venomotion

In this section, the hemodynamic effects of venomotion are studied by examining the parameter variation, pressures, and flows in the vascular region bounded by the pressures P_5 and P_{10} as shown in fig. 4.10. The results reflect the simultaneous solution to all the model equations of Chapter Four, Section V-B, with the exception of the parametric control of precapillary sphincter dynamics given by eq. 4.26. (This aspect will be taken up in Section B).

1. Parameter Variation as a Function of Effective Wall Stress

As was decribed in Chapter Four, Section III-B, the left hand side of equation 4.7 represents the difference between the wall stress tending to cause the vessel to dilate and the active stress tending to cause it to contract. For convenience, we will call the net stress tending to dilate the vessel the effective wall stress (S_e). In the results shown in fig. 5.2, the effective stress is the driving function responsible for the resultant parameter variation. Onset of muscle contraction is shown as a reduction in S_e, since an increase in muscle contraction reduces the effective stress tending to dilate the vessel. In the example shown in fig. 5.2, the contraction phase lasts for one second, at which time the force developed by the muscle decreases to its basal tone level in a linear fashion, and at a slower rate than that which it developed that force.

Figure 5.2 shows the time relationship between the simulated muscle contraction, and resultant effective wall stress (S_e) and the

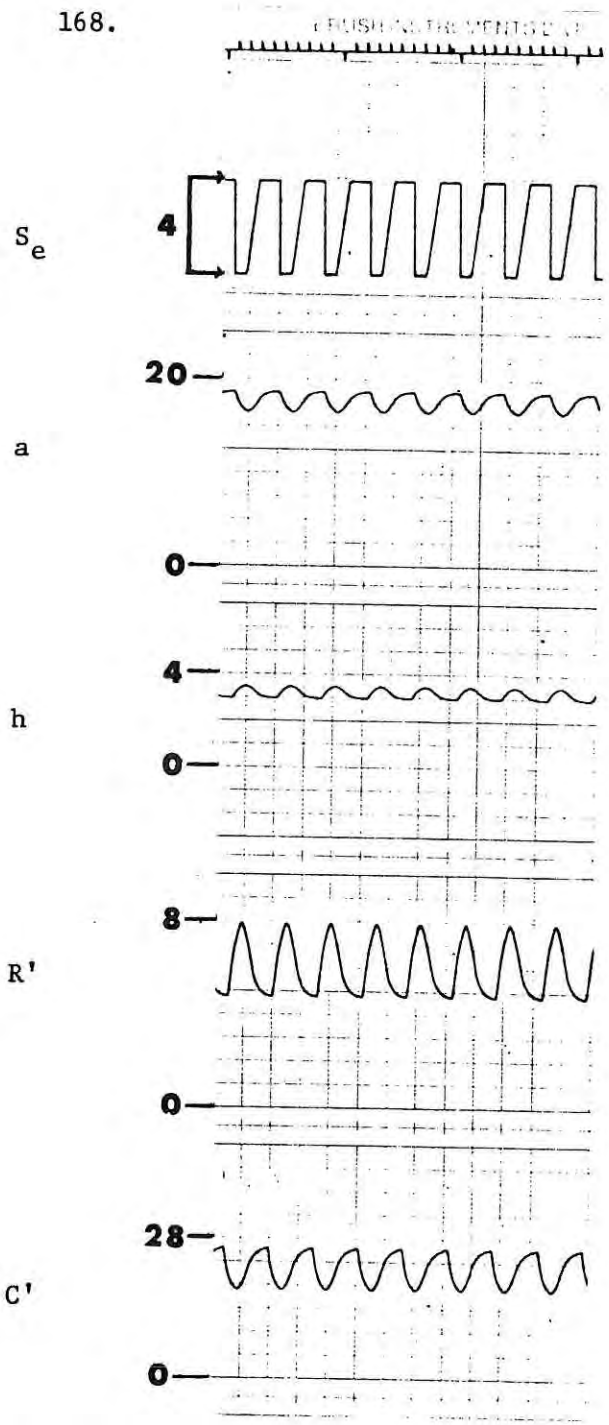

Figure 5.2 Parameter Variation. The time variation of vessel radius (a), wall thickness (h), segmental resistance (R'), and segmental compliance (C'), associated with simulated muscle contraction (S_e). Units: a and h in microns; R in 10^8 dynes sec cm^{-5}; C in 10^{-12} $dynes^{-1}$ cm^5 and effective stress, S_e, in units of 10^5 dynes cm^{-2}. Time marks at top are at one second intervals.

effect on internal radius (a), wall thickness (h), segmental resistance (R), and segmental compliance (C). Muscle contraction initiates a reduction in internal radius and a simultaneous increase in vessel wall thickness. The immediate consequence is an increase in segmental resistance and decrease in compliance. When relaxation occurs, all parameters are seen to return toward their resting levels.

2. Hemodynamics with No Imposed Pressure Gradient

In order to evaluate the intrinsic "pumping" characteristics of the active vessel, a set of simulations were carried out in which the upstream arterial pressure P_o and the downstream venous pressure P_v were made equal and the branch flow, $Q_b(t)$, was made zero. This meant that all observed hemodynamics were strictly due to the dynamic variation of the active vessel diameter. The results of these simulations are separated into two major categories for clarity of presentation. The first category is that corresponding to a contraction mode in which all segments alter diameter simultaneously. This mode of contraction is referred to as uniform contraction. The second mode of diameter variation is that corresponding to a simulated contraction wave propagating along the length of the vessel in the direction from P_5 to P_{10}. In this mode, the first upstream segment (region between P_5 and P_6) is the first to contract. After a controllable time delay, the second segment contracts, then the third, and so on until all segments have contracted. This mode of diameter variation simulates the so called peristaltic process described previously (Chapter Four, Section III-B).

a. Uniform Contraction

i. Pressure-Flow Relationships

Figure 5.3 is a record showing (from top to bottom) vessel radius (a), effective wall stress (S_e), small vein entrance pressure (P_5), small vein exit pressure (P_{10}), pressure difference across the active vessel ($P_5 - P_{10}$), and the flow out of the active vessel (Q_{sv_o}) and the flow into the vessel (Q_{sv_i}).

Contraction is initiated and coincides with the rise in active muscle stress. In figure 5.3, this corresponds to the rapid downward movement of the effective wall stress, (S_e). As can be seen, the contraction precipitates a reduction in radius and an elevation in pressure. The effect of the rising pressure is coupled back to the effective stress, as evidenced by the secondary rise in this quantity. Physically, this means that the pressure increase due to the contraction tends to reduce the amount by which the radius will be reduced.

The inflow is seen to decrease and the outflow to increase during the contraction period, with the reverse being true during the relaxation phase. Physically this means that during contraction blood within the vessel is expelled, some toward the arterial side, and some toward the venous side. The amount of flow decreases until the rate of change of radius approaches zero. At this instant, there is a reversal in the direction of the pressure gradient and flow direction, which means the vessel is being filled from both upstream and downstream regions.

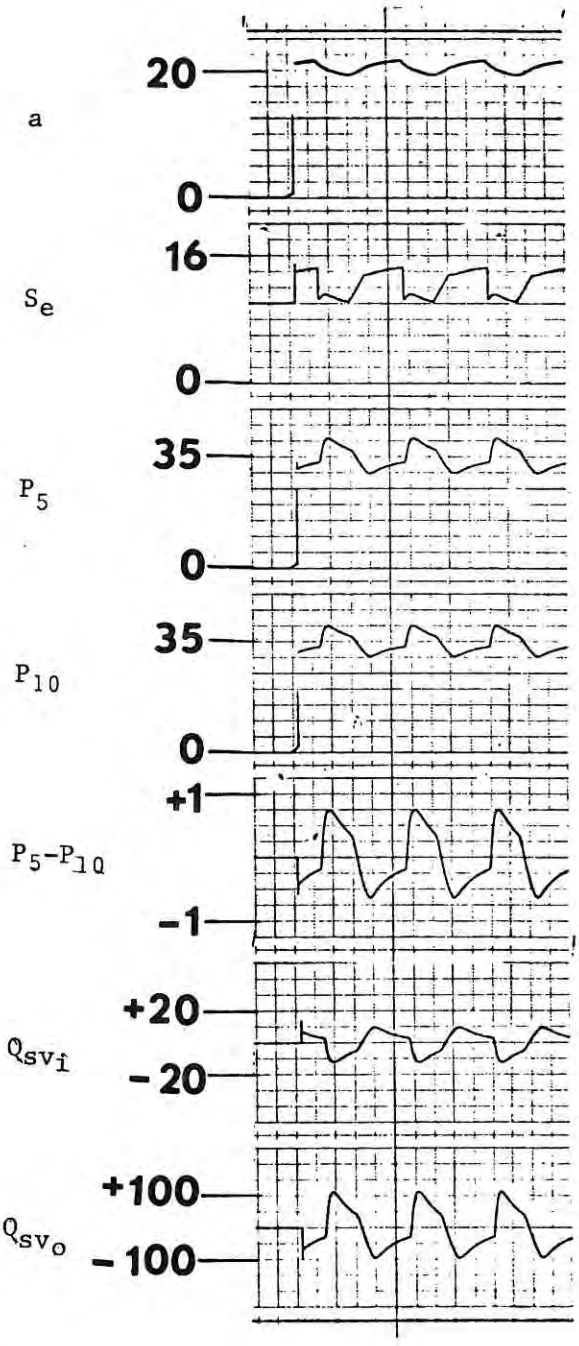

Figure 5.3. Dynamics of uniform contraction. Pressures (10^3 dynes cm^{-2}) and flows (10^{-8} cm^3 sec^{-1}) correspond to those shown in the Microvascular Model (figure 4.10). The vessel radius (a) is shown in microns and the wall effective stress (S_e) in units of 10^4 dynes cm^{-2}. The fixed end pressures (P_o and P_v) for the case shown are 35 x 10^3 dynes cm^{-2}. Each mm mark is one second.

ii. Effect of Pressure on Dynamics

In Figure 5.4, the effect of changing the absolute value of the intravascular pressure is illustrated. Figure 5.4a, b, and c correspond to arterial and venous pressures of 35, 20, and 10 x 10^3 dynes cm^{-2}, respectively. As pressure goes from 35 to 10 dynes cm^{-2}, a relaxed and contracted diameter of 14% is noted. The decrease in radius during the relaxed phase is due in part to the smaller transmural pressure acting against the vessel wall.

The amplitude of the radius change, expressed as a percentage of the maximum value at a given pressure, increases slightly with decreasing pressure. In physical terms, this indicates that for the same magnitude of muscle contraction, the fractional change in radius will be larger for smaller intravascular pressures.

Another characteristic illustrated by figure 5.4 is the increase in fractional pressure developed by the contracting vessel with decreasing intravascular pressure. Denoting the pressure at the end of the muscle relaxation period as P_R and the peak increase in pressure due to the muscle contraction as ΔP_R, then the fractional pressure developed by the contractions is $\frac{\Delta P_R}{P_R}$. These quantities are summarized in Table 5.2.

Table 5.2

Intravascular pressures developed by muscle contraction where arterial (P_0) and venous (P_V) pressures are made equal. Data is from figure 5.4 pressures in units of 10^3 dynes cm^{-2}.

Arterial and Venous Pressures ($P_0 = P_V$)	End Relaxation Pressure (P_R)	Developed Pressure (P_R)	Fractional Developed Pressure $\frac{(\Delta P_R)}{P_R}$
10	9	6	.67
20	19	6.5	.34
35	33	8	.24

From Table 5.2, the fractional developed pressure is seen to decrease with increasing and relaxation pressure, though the absolute value of the developed pressure increases. Wiederhielm (1967) recorded dynamic pressure variations which follow this general trend. For an end relaxation pressure of 7.5 mm Hg, a developed pressure of about 5 mm Hg was recorded. The model prediction for an end relaxation pressure of 9×10^3 dynes cm^{-2} (6.8 mm Hg) is 6×10^3 dynes cm^{-2} (4.5 mm Hg). The other peak to peak pressure variations of Table 5.2 are also in accord with the experimental data of Wiederhielm (1967). The significance of this developed pressure associated with contraction will be discussed below in Section iiii.

iii. Mean Flow

Evaluating the time averages of both inflow (Q_{sv_i}) and outflow (Q_{sv_o}) in figure 5.2 shows that in all cases, the time average is zero. Physically, this means that though the active diameter variation converts no flow (i.e., zero imposed pressure gradient)

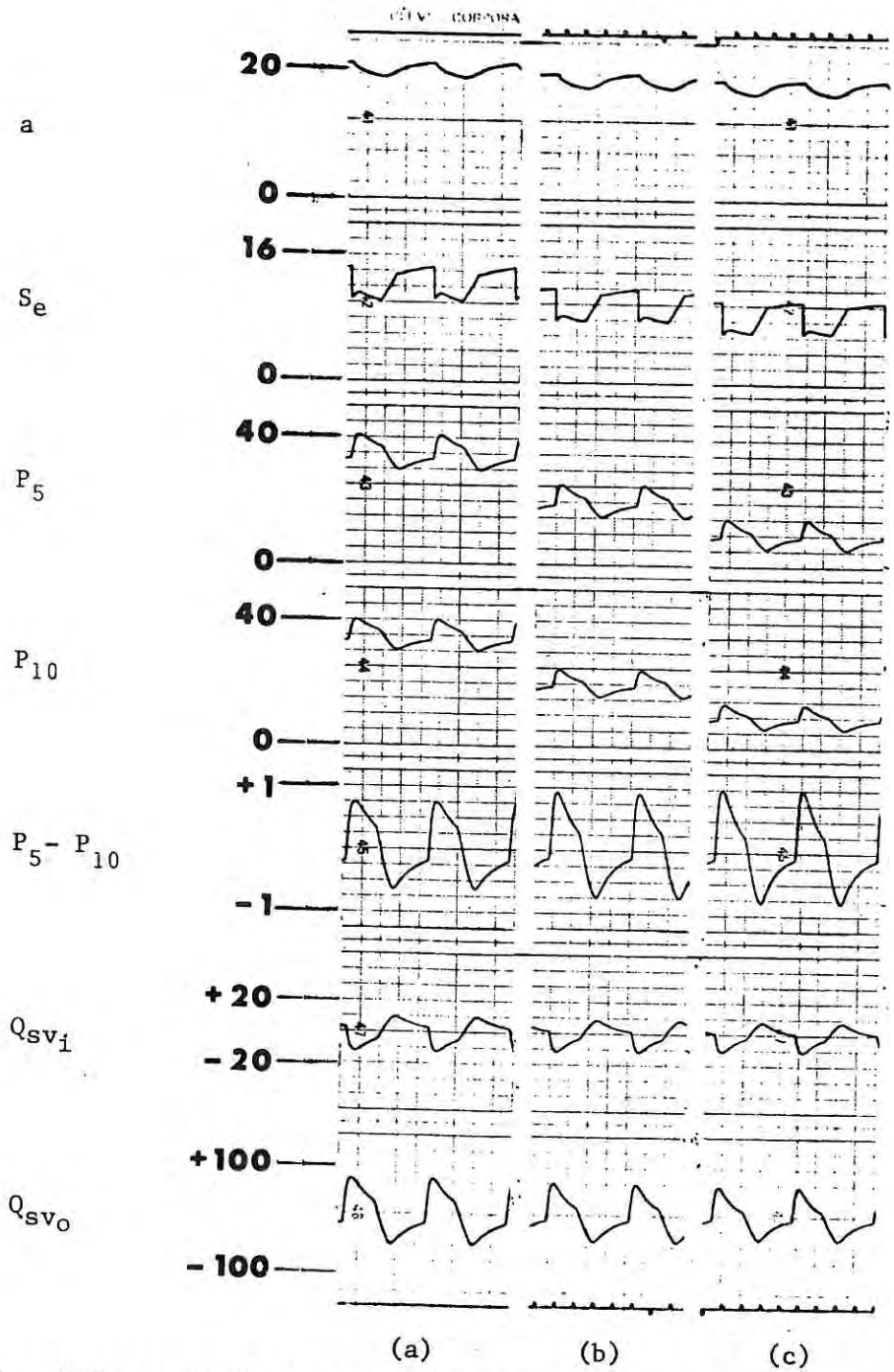

Figure 5.4. Effects of intravascular pressure on dynamics of uniform contraction. Pressures (10^3 dynes cm^{-2}) and flows (10^{-8} cm^3 sec^{-1}) correspond to those shown in figure 4.10. Vessel radius (a) is in microns and wall effective stress (S_e) in units of 10^4 dynes cm^{-2}. Each mm mark is one second. In (a), (b) and (c) the fixed arterial and venous end pressures are 35, 20 and 10 x 10^3 dynes cm^{-2}, respectively.

into a periodic flow, the net result averaged over a cycle is zero. It may thus be concluded that uniform, periodic diameter variation is not an effective "pump" in the sense of producing a net mean flow, in the absence of an imposed pressure gradient for the case just considered.

iiii. Effect of Values

A reason for the zero average flow found above may be that the valve simulation (equations 4.16 & 4.17) has not yet been incorporated, thus permitting bidirectional flow. In order to test the significance of these valves with respect to the generation of a non-zero flow, the vessel hemodynamics corresponding to flow over the entire cycle have been compared to one in which flow occurs only during contraction. In this formation, the developed pressure (Section iii) due to contraction, simulates the driving pressure to open and close the valves. Typical results are shown in fig. 5.5, in which the effect of including the valves (b) is compared with results obtained when they are not included (a) in the simulation. Without the valves, the pressure is seen to oscillate around the fixed end pressure (40×10^3 dynes cm^{-2}). With the valves simulated, the fixed end pressure is obtained during the relaxation phase followed by an increase of almost 25% associated with contraction. It may also be seen that the zero mean flow associated with the result of (a) is converted to a non-zero mean flow by the valve presence. Thus, given the presence of the valves, the uniform contraction gives rise to a net outflow.

In order to investigate the effect of different contraction durations and frequencies on the amount of mean flow so generated, a variety of muscle contraction forms were simulated, and pertinent

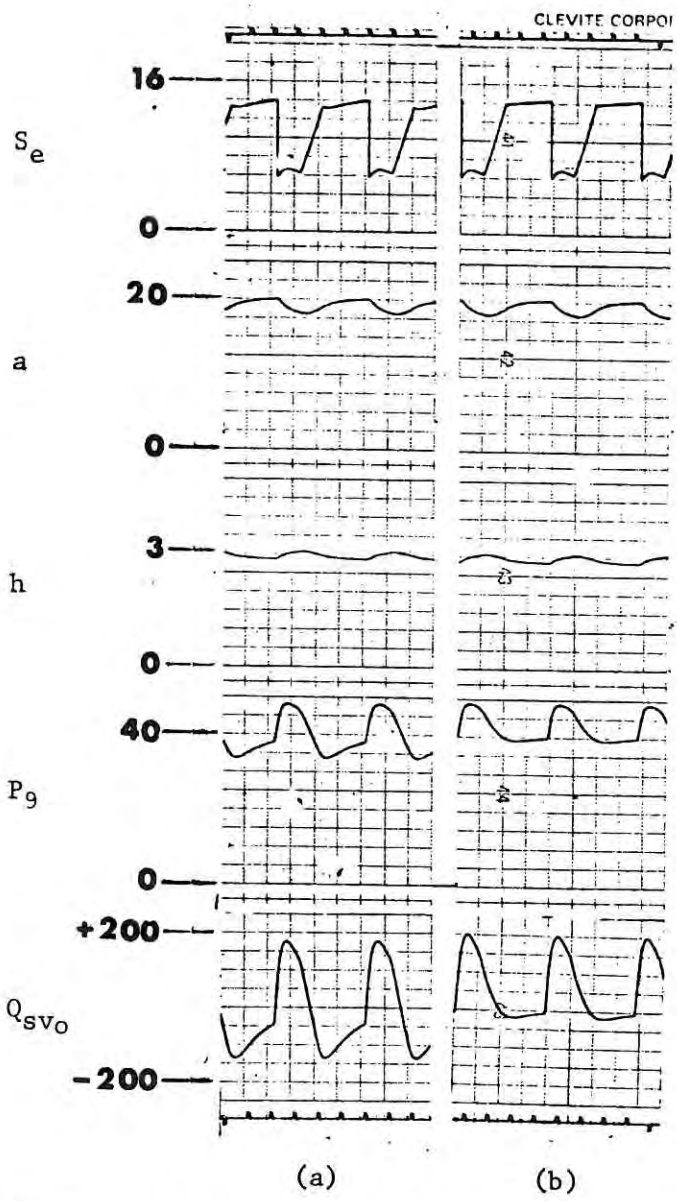

Figure 5.5. Effect of valves on dynamics. Pressure (10^3 dynes cm^{-2}) and flow (10^{-8} cm^3 sec^{-1}) correspond to those shown in figure 4.10. Wall thickness (h) and inside radius (a) in microns. Effective wall stress (S_e) in units of 10^4 dynes cm^{-2}. Time marks at one second intervals. Fixed end pressure is 40 x 10^3 dynes cm^{-2}. In (a) without valves and in (b) with valves.

quantities recorded. Figure 5.6 displays some representative values of the effective stress and outflows recorded. In 5.6a through 5.6d, the fundamental period of contraction is 4 seconds. This corresponds to a commonly observed in vivo rate (Chapter Six). The contraction durations are respectively (a to d) 2, 1, .5 & .25 seconds. In e, the fundamental period is reduced to 2 seconds and the contraction duration is .5 seconds.

From these results, the mean flow vs. contraction duration is plotted in figure 5.7. The results indicate that for a given fundamental period (in this case, 4 seconds), the mean flow which is attributable to the active vessel "pumping" increased with increasing contraction duration. From figure 5.7, it may be seen that a contraction duration above about 1 second does not further increase flow, whereas between .2 and 1 second, there is almost a linear relationship. The explanation for the flow saturation or plateau is related to the fact that for contraction durations above about 1 second, there is no further decrease in the vessel radius. For this contraction time, the vessel radius achieves a new equilibrium value which reflects the balance of forces between the now prevailing transmural pressure and the contracted state of the muscle. Due to the viscoelastic properties of the wall, however, if the contraction time is less than about 1 second, then there is not sufficient time for the radius to achieve its contracted equilibrium state. Thus the longer the contraction duration, the greater the reduction in radius, and consequently an increase in flow.

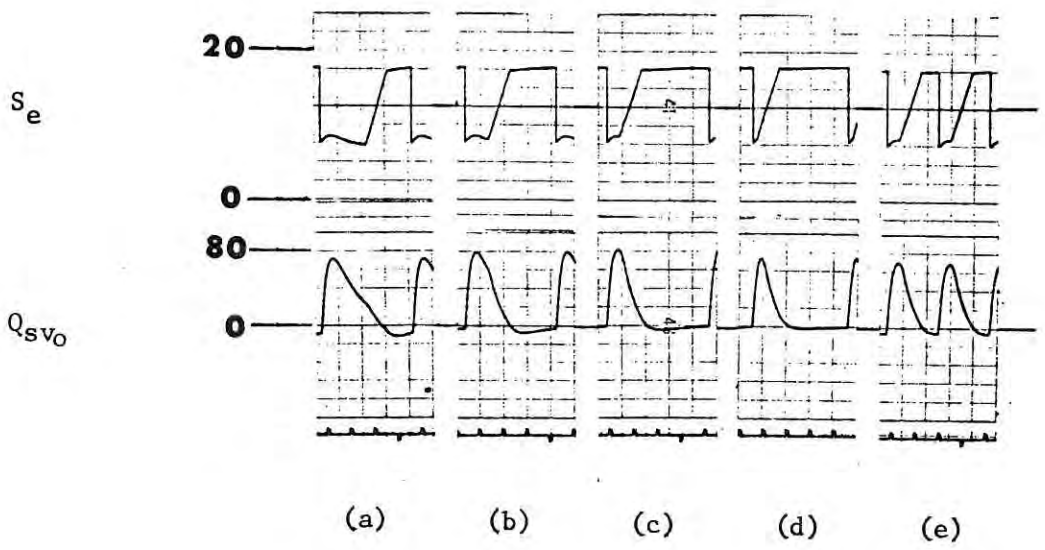

Figure 5.6. Effect of contraction duration and frequency on flow. Effective stress (S_e) in units of 10^4 dynes cm^{-2} and active vessel outflow (Q_{sv_o}) in units of 10^{-8} cm^3 sec^{-1}. Time marks at one second intervals. In (a) through (d) the fundamental period is four seconds, and contraction durations are, respectively, 2, 1, .5 and .25 seconds. In (e) the fundamental period is two seconds, and the contraction duration is .5 seconds.

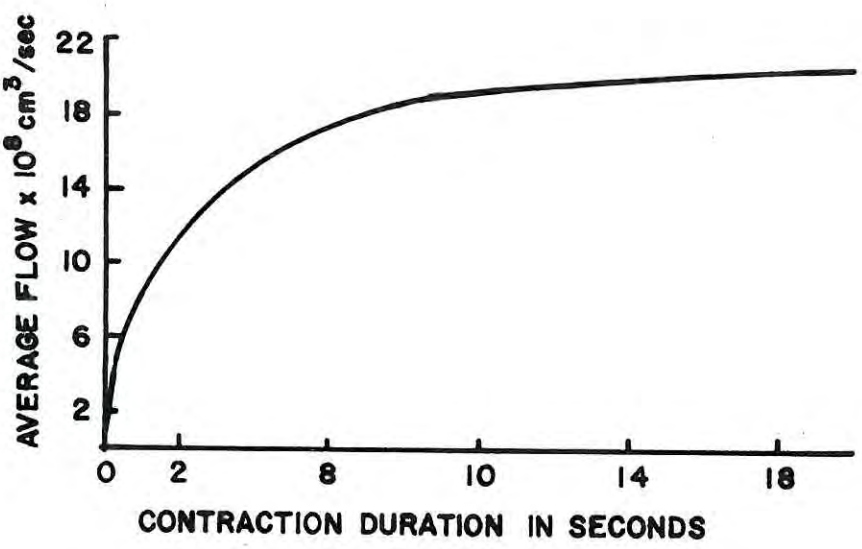

Figure 5.7. Mean flow as a function of contraction duration. Fundamental period is four seconds.

It is interesting to note that in the experimental observations (Chapter Six) on these vessels in vivo, measured contraction times have been in the range of .5 to 1 second for all frequencies observed. Thus, for example, when the venomotion period was caused to decrease (either by temperature or pressure stimuli) from 4 to 2 seconds, the contraction duration remained within its original range, whereas the relaxation duration was significantly reduced.

The effect of changing the fundamental period on flow is illustrated in figure 5.6e. The frequency is double that of part c of this figure, but the contraction time is the same. The flow per cycle is slightly less at the higher frequency, but because there are now flow pulses in a time increment which had only one in the low frequency case, the average flow is almost twice as large (25×10^{-8} cm^3/sec).

b. Non-Uniform Contraction

i. Pressure-Flow Relationships

The effect of non-uniform contraction on vessel hemodynamics is illustrated in figure 5.8. The top panel is the pressure at the active vessel entrance (P_5), the middle panel is the pressure difference across the entire active vessel ($P_5 - P_{10}$), and the bottom panel is the outflow (Q_{sv_o}).

Figure 5.8a corresponds to a segment delay in time (δ) of 0, i.e., uniform contraction; in b, (δ) = 100 msec; in c, (δ) = 200 msec; in d, (δ) = 400 msec; and in e, (δ) = 800 msec. In all cases $P_0 = P_v = 20 \times 10^3$ dynes cm^{-2}.

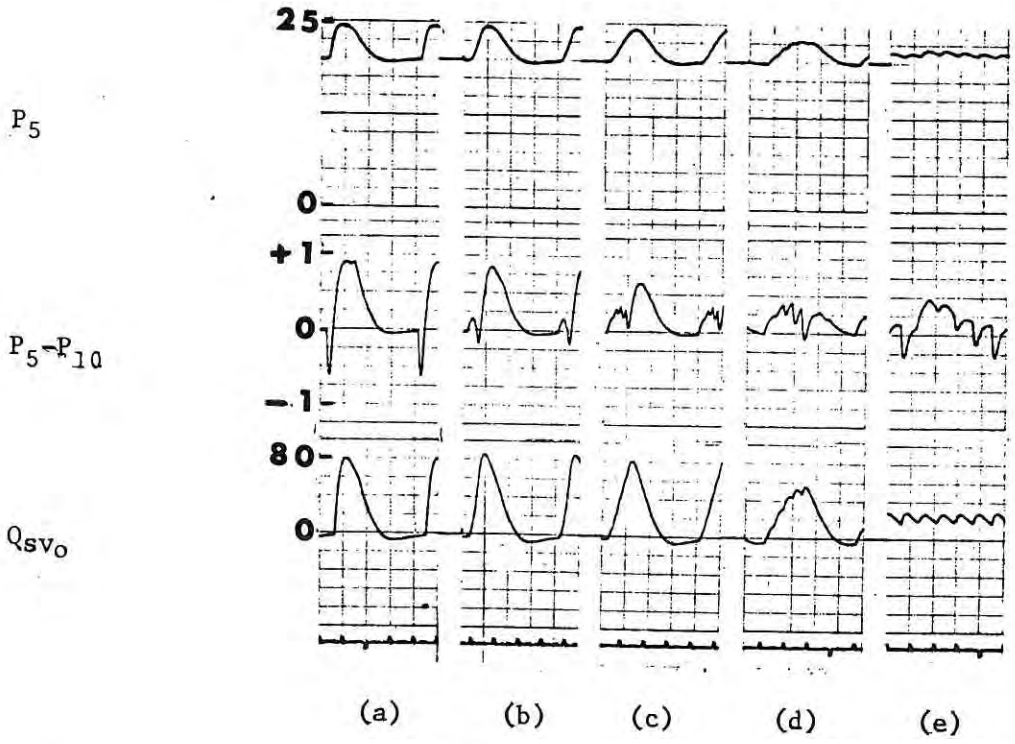

Figure 5.8. Hemodynamics of non-uniform contraction. Pressures (10^3 dynes cm^{-2}) and flows (10^{-8} cm^3 sec^{-1}) correspond to those shown in the Microvascular Model of figure 4.10. Time marks at one second intervals. Fundamental period of venomotion is four seconds. Panels (a), (b),(c), (d), and (e) correspond to segment delays (δ) of 0, 100, 200, 400 and 800 msec, respectively.

Referring to figure 5.8, the difference between the intravascular pressure waveforms obtained for uniform contraction as compared with non-uniform contraction increases with increasing segment delay time. In the case of uniform contraction ($\delta = 0$), all segments contract together and produce a pressure peak of about 5×10^3 dynes cm^{-2}. For delays up to (but not including) 400 msec, the individual contributions to pressure elevation are not discernable in the pressure waveform. However, the effect of the delay is seen by the decrease in the rate of rise of the developed pressure. At a delay of 400 msec (d), there becomes sufficient resolution to actually see that the developed pressure is really due to sequentially contracting segments. The separate effects are more clearly seen in the pressure difference (middle panel). For example in (d), the contraction of the first segment gives rise to a developed pressure difference of about 255 dynes cm^{-2}. Since the muscle contraction time for this simulation is 100 msec, the second segment contraction begins while the first segment is in the contracted state and gives rise to a developed pressure difference peak of about 150 dynes cm^{-2}, which is added to that due to the first segment. By the time the third segment is to contract, the pressure developed due to the first contraction has decreased, and is still decreasing. However, when the third segment contracts the pressure is again augmented. This process continues until the final segment contracts by which time the pressure developed due to the preceding contractions has already fallen to its

minimum value. The final segment contraction results in a developed pressure difference of about 300 dynes cm^{-2}. After contraction of the final segment, there is a time interval for which the vessel is free from contraction and the pressure falls.

In figure 5.8e, this contraction free interval is reduced to zero by using a segment contraction delay of 800 msec. With the muscle contraction time of 1000 msec used in this simulation, this means that successive contractions occur while the immediately preceding segment is in a contracted state and that contraction will occur over the entire fundamental period of four seconds. The result of this continuous reinforcement as seen in (e) (top panel) is to reduce the pressure variation due to individual segment contractions. This has the effect of producing roughly the same average pressure as the uniform contraction but a significantly reduced peak to peak variation.

ii. Mean Flow

The outflow from the active vessel is shown in the bottom panel of figure 5.8. The average flows calculated for figure 5.8a through e respectively are 19, 19.5, 20, 21, 22.5 x 10^{-8} ml/sec. From these calculations, it is clear that there is some dependence of the developed flow on the segment contraction delay. However, with respect to the flow developed by purely uniform contraction ($\delta = 0$), the additional flow due to contraction wave propagation is small.

3. Hemodynamics With Imposed Pressure Gradient

a. Pressure-Flow Relationships

As has been previously mentioned, venomotion frequencies in the range of .1 to .5 Hz have been experimentally observed. In figure 5.9 the steady state hemodynamics associated with three venomotion frequencies (uniform contraction) are illustrated as obtained from the simulation. Figure 5.9a, b, and c correspond to venomotion frequencies of .25 Hz (T = 4 sec.), .33 Hz (T = 3 sec.) and .5 Hz (T = 2 sec.) respectively. The variables displayed correspond to selected pressures and flows as indicated in the Microvascular Model. A word of explanation concerning the display of the time average flows is in order. As depicted Q_{sv_i} & Q_{sv_o} represent the "running" average. That is, the instantaneous value of flow is averaged continuously and displayed. After a passage of time corresponding to the fundamental venomotion period, the value corresponds to the flow average over one cycle. The averaging system is then reset (seen as a vertical line in the figure) and the process repeated. The addition of the imposed pressure gradient maintains a non-zero mean flow over the entire venomotion cycle. One of the consequences of this is that the hemodynamic variables appear "smoother" than was seen for the case of zero imposed pressure gradient (c.f., Q_{sv_o} of fig. 5.9 and Q_{sv_o} of of fig. 5.4)

In fig. 5.9a, the onset of contraction is seen to precipate a decrease in the inflow and an increase in the outflow. The reduction in the inflow is attributable to two events which occur simultaneously.

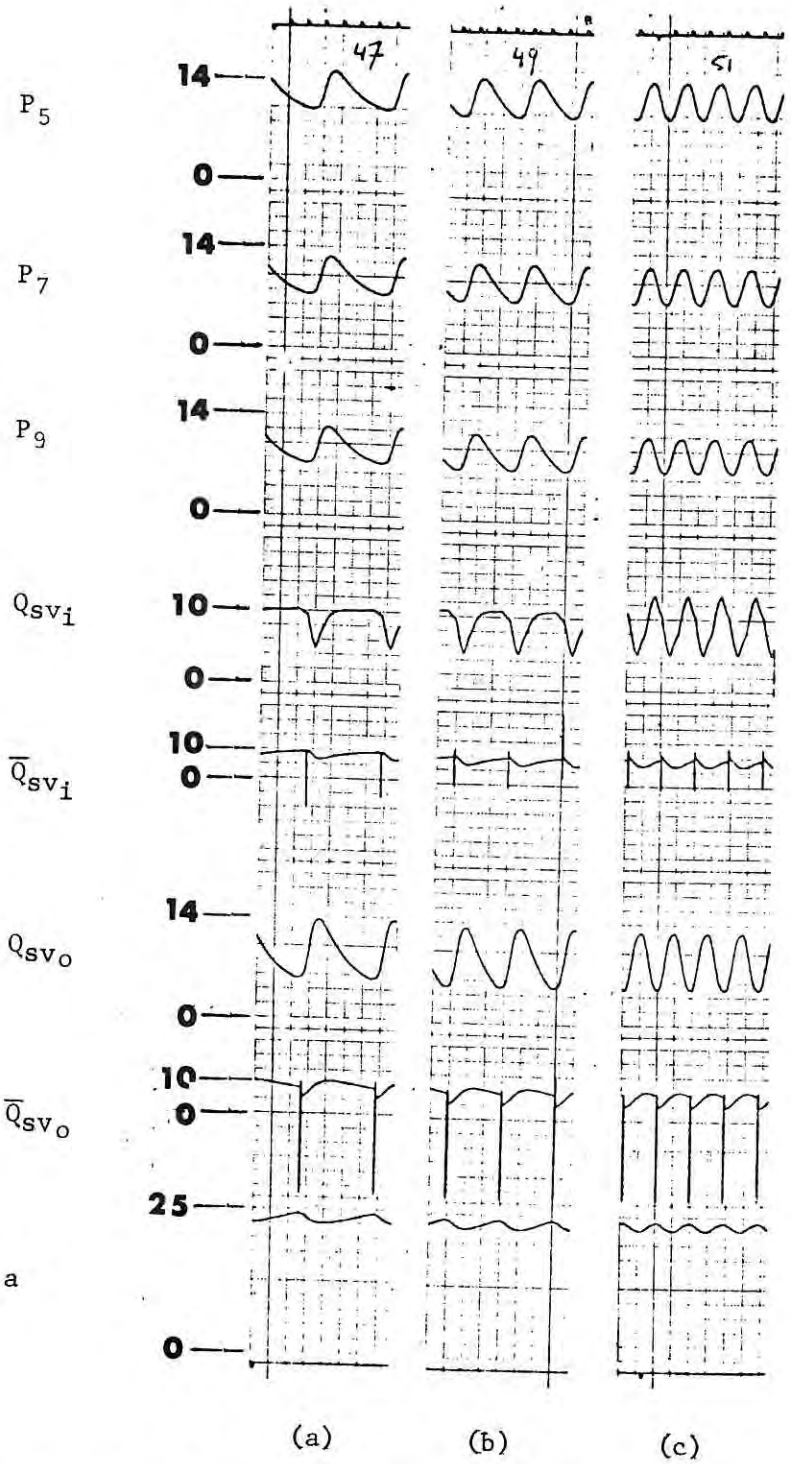

Figure 5.9. Hemodynamics with imposed pressure gradient and uniform contraction. Pressures (mmHg) and flows (10^{-7} cm^3 sec^{-1}) correspond to those in figure 4.10. Bar over quantity denotes running average. Radius, a, in microns. Time marks at one second intervals. In (a) fundamental venomotion period, T_V = 4 seconds; in (b), T_V = 3; and in (c), T_V = 2 seconds.

The reduction in radius associated with the contraction increases the hydraulic impedance at the entrance to the vessel, and thus contributes to the flow reduction. Additionally, the contraction process reduces the vessel fluid volume. A portion of the expelled volume results in a back flow toward the capillary, as was shown in the analysis with zero imposed pressure gradient. In the present case, that is, with a non-zero imposed pressure gradient, this "reverse" flow component is measured as a flow reduction in the vessel inflow. Because the source resistance, as seen by the active vessel, is large compared to the downstream resistance, the reduction in inflow due to the increase in hydraulic resistance per se is small compared with the effect of the active flow mechanism. This active flow (i.e., that generated by the contraction process and simultaneous reduction in segmental compliance) is roughly dominated by the rate of change of vessel radius. Thus, the inflow will continue to decrease, but at a decreasing rate until the rate of change of radius is approximately zero, at which time the inflow should be about at its precontraction level. This time relationship is apparent, for example in fig. 5.9.

The rise in the outflow is due to the expulsion of the fluid volume and concomitant decrease in the segmental compliance. The outflow continues to rise, but also at a decreasing rate until the rate of change of radius is approximately zero. It is at this point that the peak outflow occurs, and after which the outflow begins to decrease. The peak outflow corresponds approximately in time to the peak in the intravascular pressures.

By the time the radius begins to increase from its minimum value, the inflow has already returned to its precontraction level, and the outflow at this point in time is approximately equal to the inflow. As the vessel continues to dilate, a portion of the inflow serves to provide the fluid volume demanded by the increasing vascular volume, and the outflow falls below the inflow. However, as may be noted from the average values of inflow and outflow, the average inflow equals the average outflow, which of course is demanded by considerations of flow continuity, and is indeed satisfied.

b. Effects of Non-Uniform Segmental Contraction

Figure 5.10 illustrates the effect of different simulated contraction velocities on vessel hemodynamics. The fundamental period of venomotion is 4 seconds, and the segment delays are 0, 200, 400 msec for fig. 5.10a, b, and c respectively.

The effect of increasing delay (decreasing contraction velocity) is seen to decrease the rate of rise of the intravascular pressures and flows during the contraction phase, while simultaneously causing a spreading effect. Again, this phenomenon is due to the relative summation of the individual contractile segments. The more they act in unison, the greater will be the rate of rise of the hemodynamic variables and the smaller their dispersion.

In addition to the shape change, there is also a reduction in both pressure and flow peak to peak amplitudes, the pressure and flow peaks being smallest for the largest segment delay. However, in each case, the average vessel inflows and outflows remain the same and equal

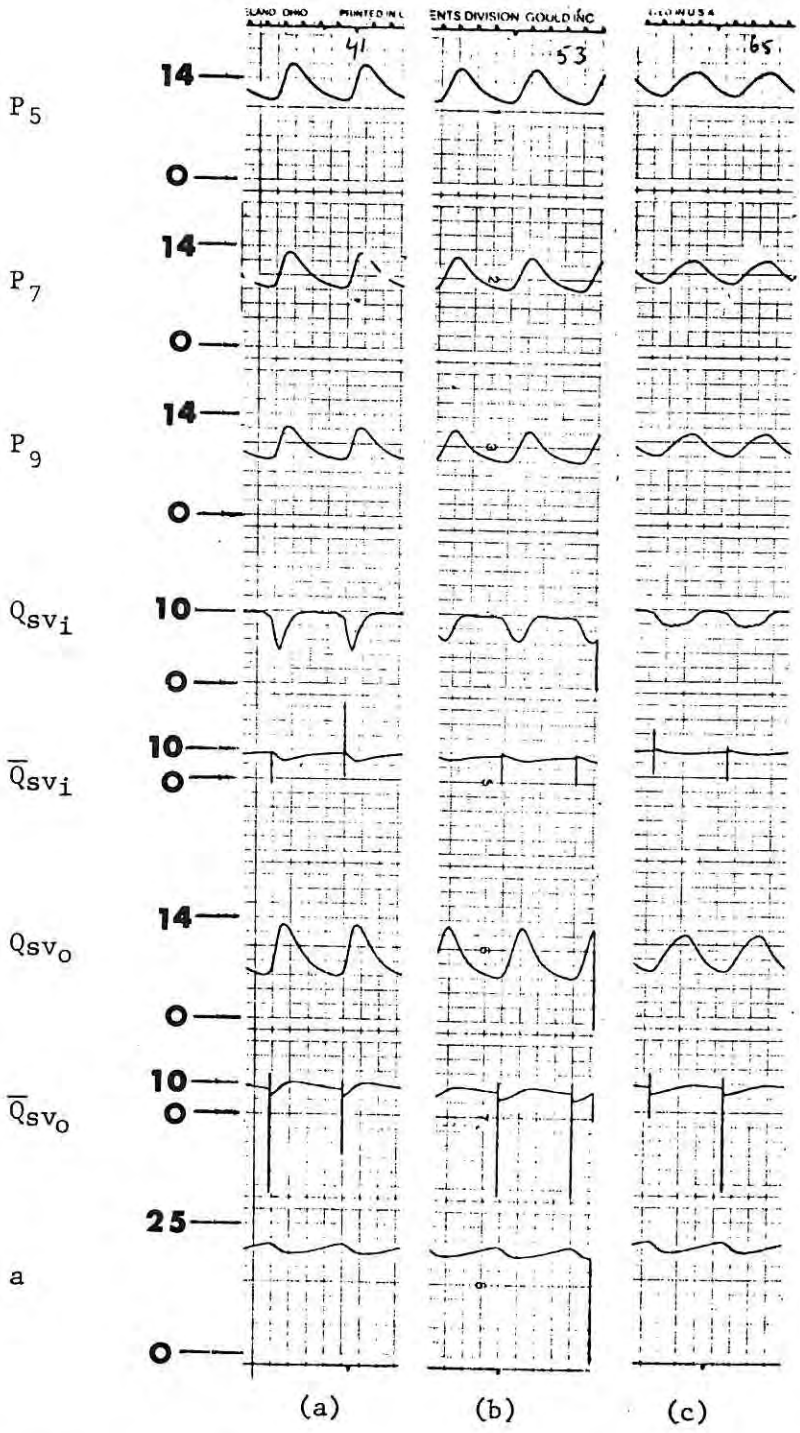

Figure 5.10. Hemodynamics with imposed pressure gradient and non-uniform contraction. Fundamental period of four seconds. Pressures (mmHg) and flows (10^{-7} cm^3 sec^{-1}) as shown in figure 4.10. Radius, a, in microns. Time marks at one second intervals. Bars denote average quantities. Segment delays in (a), (b) and (c) are, respectively, 0, 200 and 400 msec.

to each other.

In fig. 5.11, the same variables as in fig. 5.10 are displayed, but the fundamental venomotion period is in this case 3 seconds. No significant differences in the hemodynamic quantities are apparent. However, in fig. 5.12, which corresponds to a venomotion period of 2 seconds, a major change in pressures and flows associated with a time delay of 400 msec is strikingly apparent. Thus, in figure 5.12c, the time variation of the monitored hemodynamic variables is strongly attenuated, though the mean values of pressure and flow are maintained. Since the magnitude of the contraction is the same in all cases, it appears that the resultant hemodynamics are a result of the interaction of venomotion frequency, contraction wave speed, and possibly fluid velocity propagation time.

c. Intrasegmental Flow

In fig. 5.13, the relationship between the pressure, vessel inflow, and axial flow in a segment of the active vessel is illustrated. Panels a, b, and c show the effect of segmental contraction delays (0, 200 and 400 msec respectively) for a fixed fundamental period of four seconds. Panels c, d, and e show the effect of fundamental period (4, 3 and 2 seconds respectively) for a fixed contraction delay of 400 msec.

In a through c, the reduction in both the rate of change and peak values of pressure and flow with increasing contraction delay is again seen. In c through e, the dramatic effect of increasing venomotion frequency on the time course of the intrasegmental axial

flow is quite apparent. Decreasing the fundamental venomotion period from four (c) to three (d) seconds principally affects the relaxation phase of the axial flow, producing a more rapid and continuous rise in flow following contractions. Decreasing the fundamental period to two seconds (2) results in attenuation of all the hemodynamic variables in the manner already described (Section 3.b).

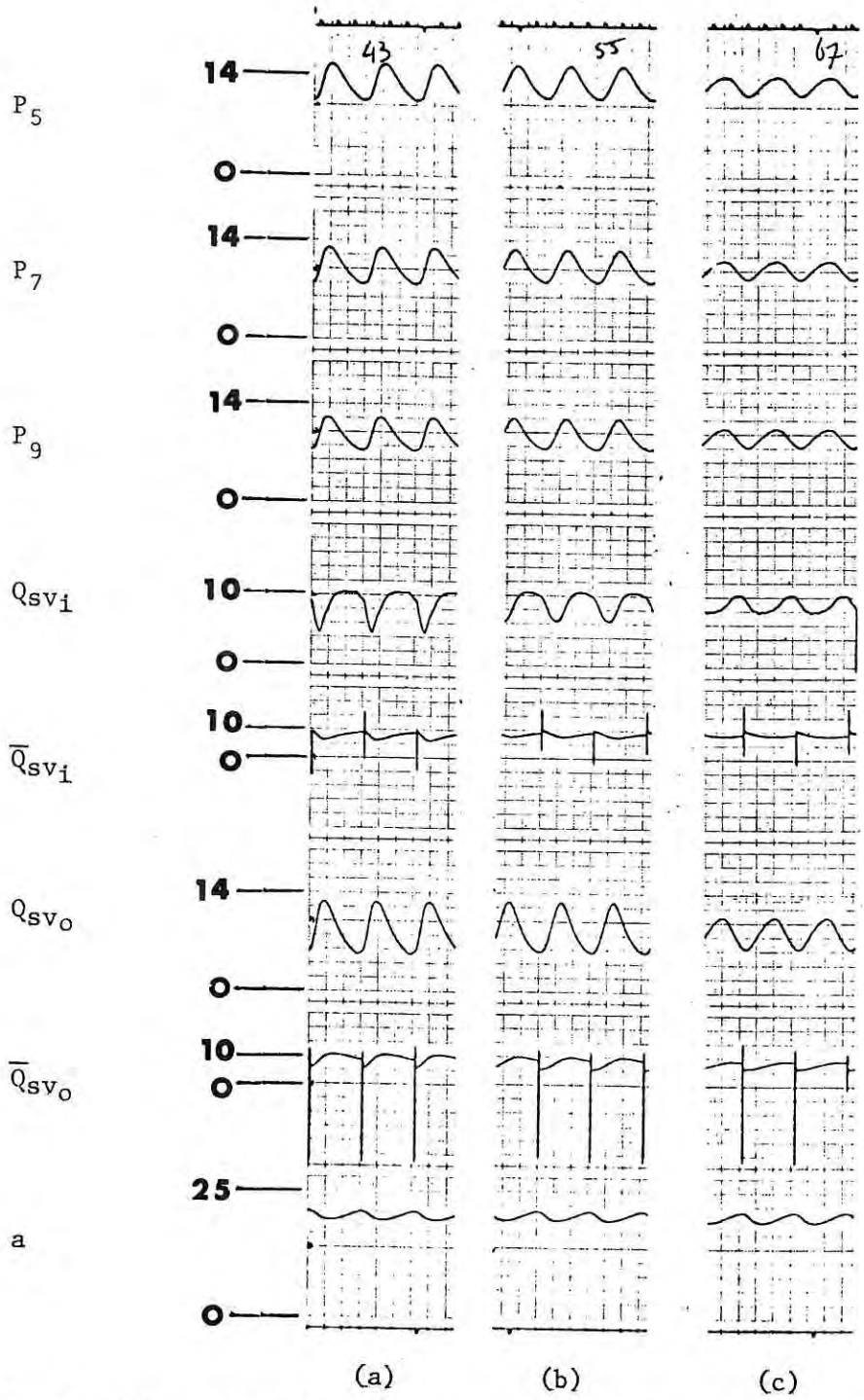

Figure 5.11. Hemodynamics with imposed pressure gradient and non-uniform contraction. Fundamental period of three seconds. Pressures (mmHg) and flows (10^{-7} cm^3 sec^{-1}) as shown in figure 4.10. Radius, a, in microns. Time marks at one second intervals. Bars denote average quantities. Segment delays in (a), (b) and (c) are, respectively, 0, 200 and 400 msec.

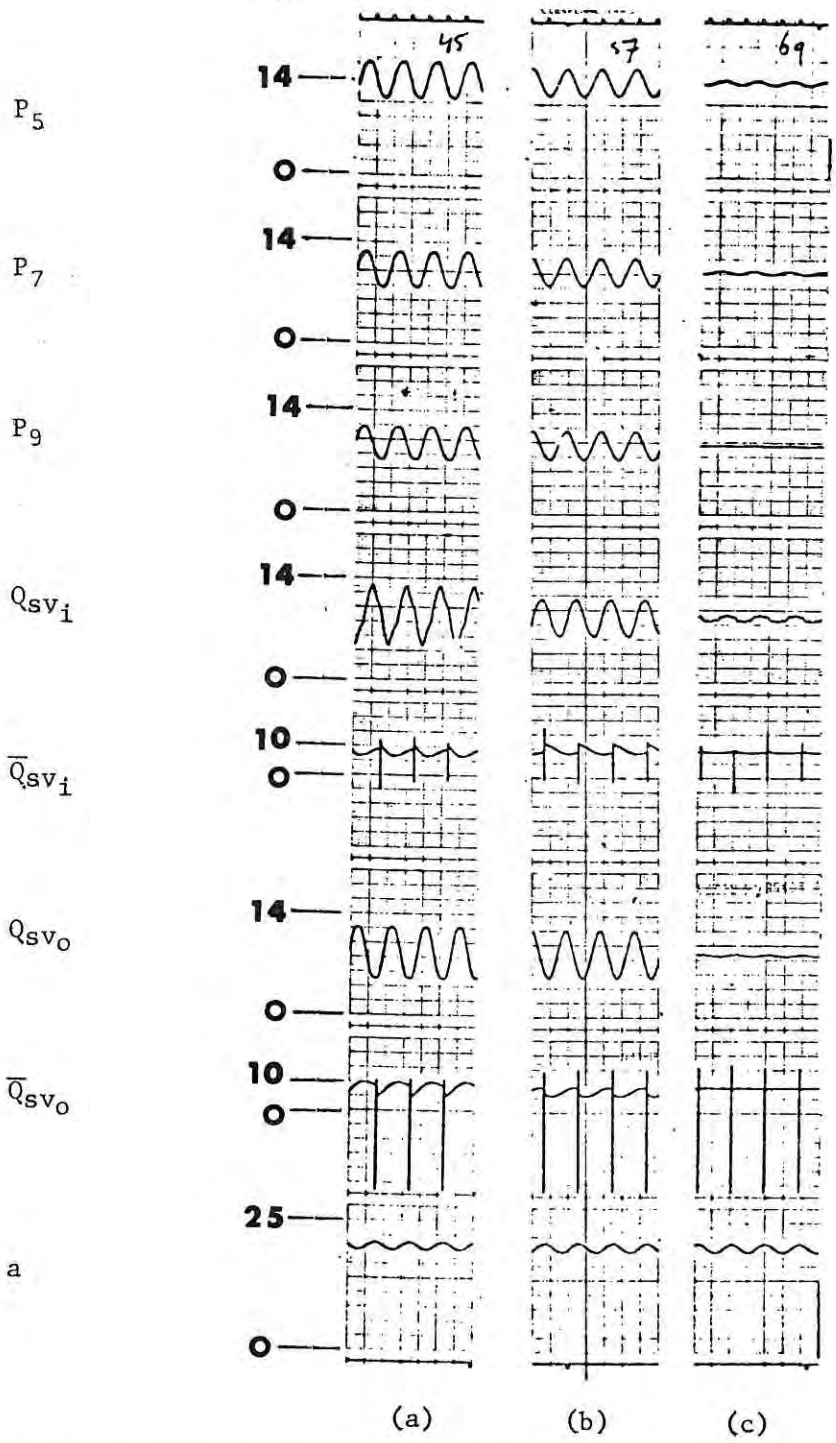

Figure 5.12. Hemodynamics with imposed pressure gradient and non-uniform contraction. Fundamental period of two seconds. Pressures (mmHg) and flows (10^{-7} cm^3 sec^{-1}) as shown in figure 4.10. Radius, a, in microns. Time marks at one second intervals. Bars denote average quantities. Segment delays in (a), (b) and (c) are, respectively, 0, 200 and 400 msec.

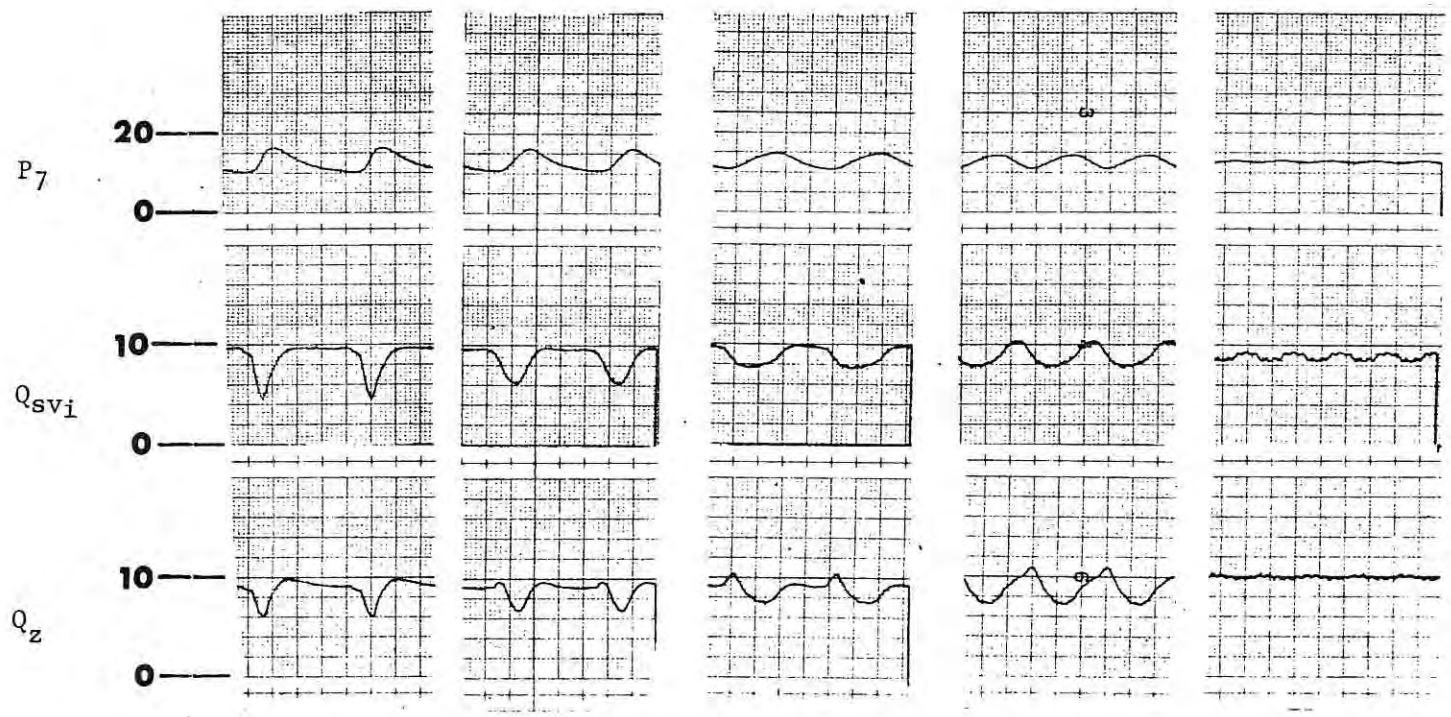

Figure 5.13 Intrasegmental Flow. Relationship between pressure, vessel inflow, and axial flow in a segment of the active vessel is illustrated. Panels a,b,and c show the effect of segmental contraction delays (0, 200, and 400 msec. respectively) for a fixed fundemental period of four seconds. Panels c, d, and e show the effect of varying the venomotion period (four, three, and two seconds respectively) for a fixed contraction delay of 400 msec. Pressures are shown in mm. Hg. and flows in units of 10^{-7} cm^3 sec^{-1}. Each mm line is One second.

B. Interaction Between Pre and Post Capillary Dynamics

1. Effect of Post Capillary Dynamics on Capillary Flow

In figure 5.14, the relationship between the small vein pressure, capillary instantaneous flow, and average capillary flow is shown. Panels (a), (b) and (c) correspond to a fundamental period of four seconds and contractions delays of 0, 200 and 400 msec respectively. Panels (d) and (e) are for non-uniform contraction with segment contraction delays of 400 msec at fundamental periods of three and two seconds respectively. The significant point to note is the inverse relationship between the capillary flow and the active pressure developed in the collecting vessel. Maximum instantaneous capillary flow occurs at the time corresponding to minimum collecting vessel pressure. It may also be noted that there is little change in the average flow in the capillary over the frequency range examined, but there is considerable reduction in the peak to peak flow and pressure variation with increasing frequency, i.e., panels (c) through (e).

2. Capillary Flow in Presence of Venomotion and Pulsatile Arterial Pressure

The effect of pulsatile arterial pressure is simulated using a sinusoidal pressure for P_0 in the Microvascular Model. For the results shown in figure 5.15, $P_0 = 50 + 10 \sin (2\pi t/T)$ with pressure in units of mm Hg. In figure 5.15 are shown (from top to bottom) pressure at the venous side of the capillary (P_4), pressure within the collecting vessel (P_7), instantaneous capillary

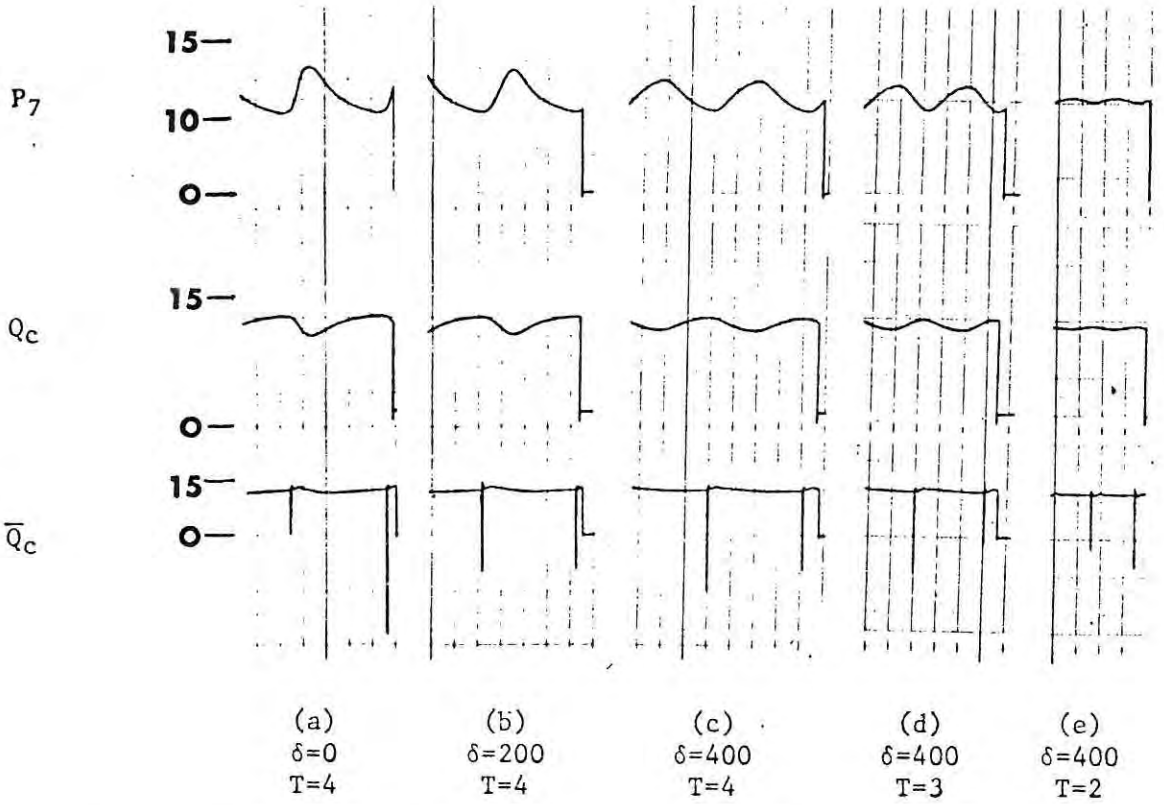

Figure 5.14. Relationship between small vein pressure and capillary flow. Pressures (mmHg) and flows (10^{-9} $cm^3\,sec^{-1}$) correspond to those of the Microvascular Model of figure 4.10. Bar denotes average. Time marks at one second intervals. T_v is fundamental period in seconds, and δ is contraction delay in msec.

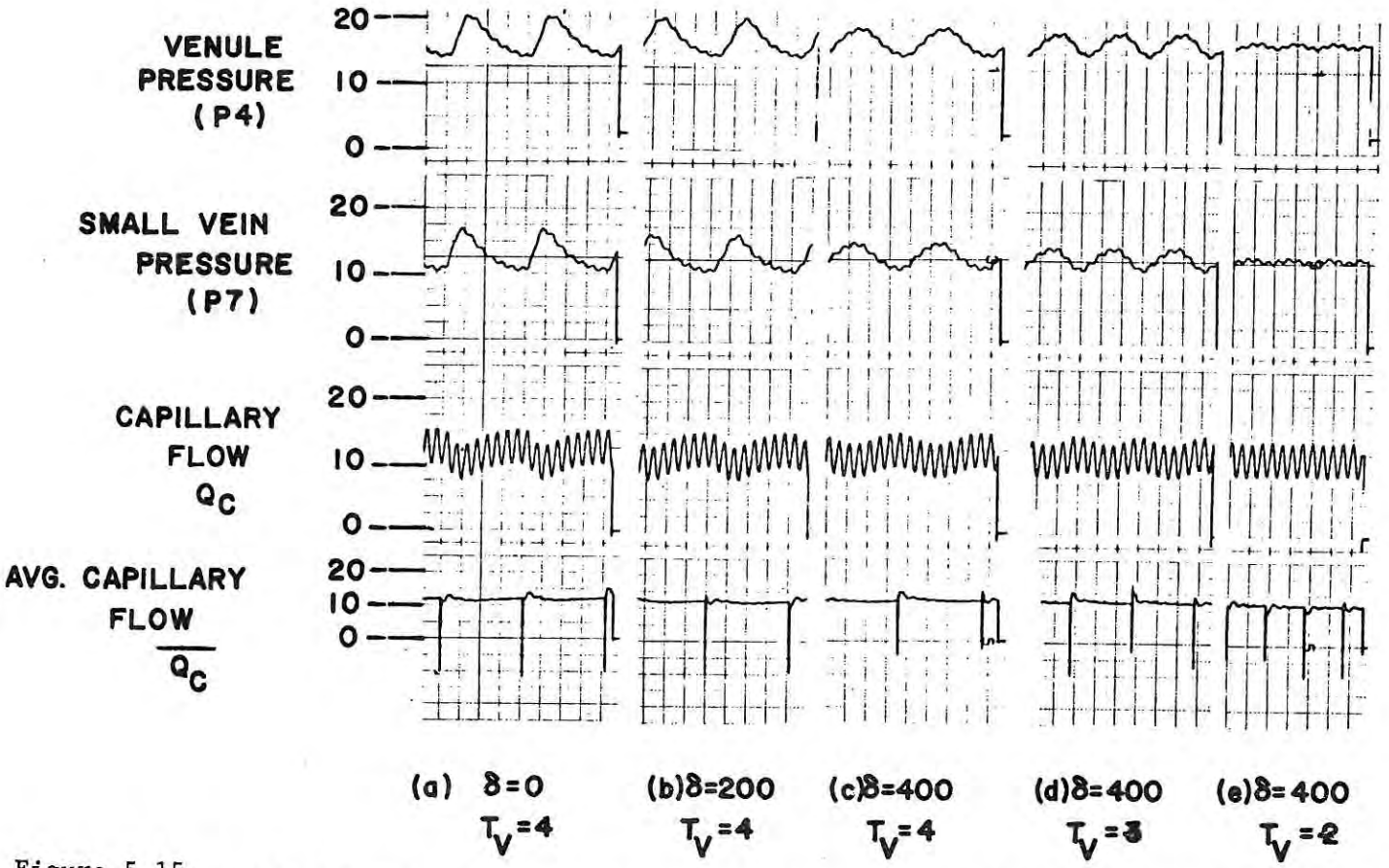

Figure 5.15.
COMBINED EFFECT OF PULSATILE ARTERIOLAR PRESSURE AND VENOMOTION ON CAPILLARY FLOW. T_V IS FUNDEMENTAL PERIOD OF VENOMOTION IN SECONDS, δ IS SEGMENT DELAY IN msec, PRESSURES IN mmHg, FLOWS IN UNITS OF $10^{-9}cm^3sec^{-1}$

flow (Q_c), and average capillary flow ($\overline{Q}_c$). Panels (a) through (e) correspond to the venomotion conditions as described in B.1 above.

There are several points to be noted in figure 5.15. First, it may be seen that there is considerable attenuation of the pulsatile pressure in passing through the capillary pathway. The arterial pulse pressure is reduced by a factor of about 24. Secondly, the pulsatile pressure variation measured at the capillary depends on the state of the active vessel. For example, in panel (a) successive arterial pulses produce smaller changes in capillary pressure as the pressure falls. This fall in pressure is associated with active vessel relaxation, and consequently a decrease in post capillary input impedance.

The capillary outflow produced by each successive arterial pulse is less sensitive to the venomotion state primarily due to the large source impedance of the single capillary pathway. Thus, the arterial related pulsatile component of capillary pressure is primarily determined by the post capillary state and the capillary outflow. In the example illustrated in figure 5.15, the range of arterial related variation in capillary pressure is from 8.5% of the arterial pulse (contracted active vessel) to 1.2% when the vessel is relaxed.

A third notable point is the magnitude of the pulsatile component of the capillary flow, which in figure 5.15 varies between 4.5 and 5.5×10^{-9} $cm^3 sec^{-1}$. The average flow calculated over a venomotion cycle is 12 in the same units. This means that the arterial pulsatile

component expressed as peak deviation from the mean capillary flow is about 2.5/12 or about 20%. This is precisely what the ratio of arterial peak to mean pressure is in the simulation, i.e., 10/50. The corresponding variation in capillary flow due only to the venomotion (uniform contraction in figure 5.15) is about 5×10^{-9} $cm^3 sec^{-1}$ for the same mean flow. Thus, in this example, the effects on the capillary instantaneous flow of arterial and post capillary dynamics are about equal in magnitude, although different in time course.

3. Dynamics Associated with Arteriole Vasomotion

a. Characteristics of Diameter Variation and Hemodynamics

As discussed in Chapter Four, Section IV-D, the arteriole vasomotion associated with local control is simulated by diameter variation of the distal segment of the terminal arteriole. This diameter variation is associated with a time variation of the effective resistance to flow through the terminal arteriole pathway in an amount which depends on the instantaneous vessel diameter.

In figure 5.16, the relationship between vessel diameter and effective resistance (R_{ta}) is shown. This figure represents the solution to equation 4.22 and serves as both a calibration of the diameter resistance correspondence and illustration of the time course of "instantaneous" resistance for a trapezoidal diameter variation.

b. Effect on Hemodynamics and Filtration

i. Uncontrolled Vasomotion

In order to examine the dynamics associated with this diameter variation and to study the effects of capillary and hemodynamic

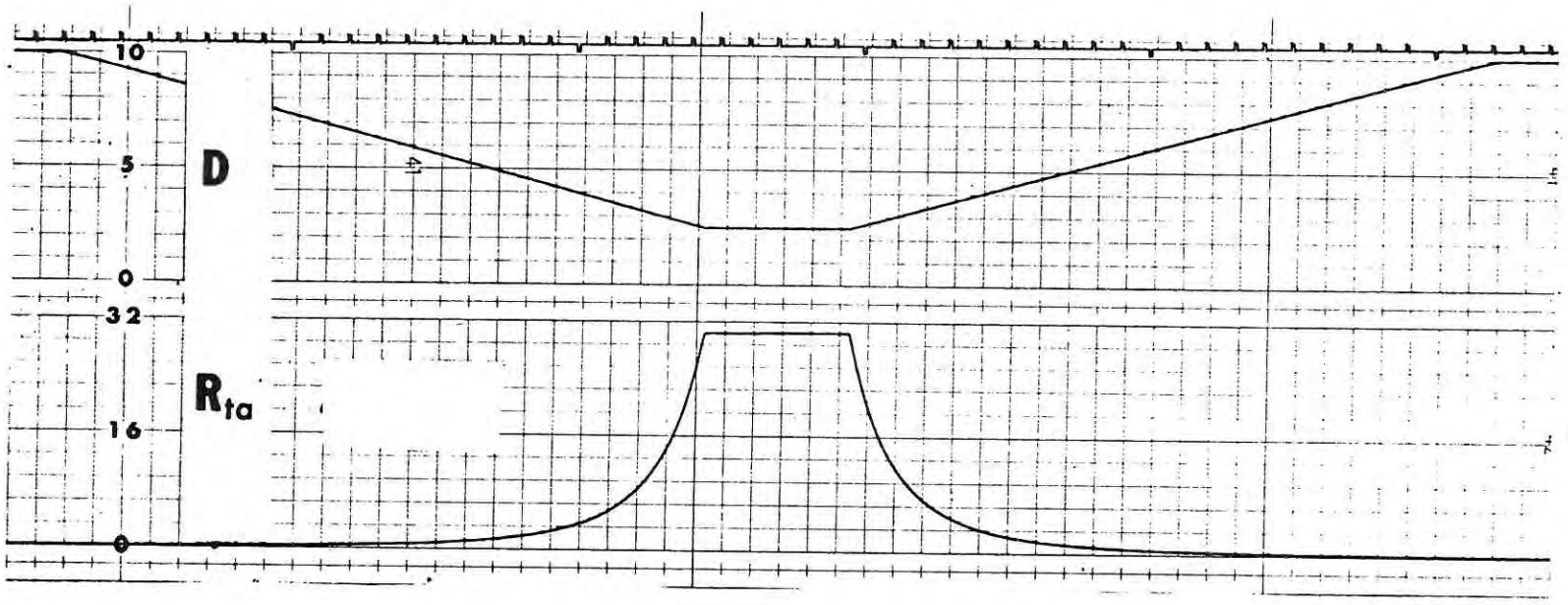

Figure 5.16. Relationship between terminal arteriole diameter and vascular resistance. D is diameter in microns, and R_{ta} is resistance in units of 10^{10} dynes sec cm^{-5}.

parameters, the diameter is initially varied in an independent fashion (i.e., time varying but independent of local control forces). This means that the control equation (eq. 4.26) is temporarily neglected. Typical dynamics are shown in figure 5.17, in which are displayed (from top to bottom): terminal arteriole diameter (D), pressure at the arterial side of the capillary (P_3), central venous pressure (P_v), instantaneous tissue pressure (P_t), time mean tissue pressure ($\bar{P}_t$), terminal arteriole flow (Q_{ta}), capillary instantaneous outflow (Q_c), and time mean capillary outflow ($\bar{Q}_c$).

Reduction in terminal arteriole diameter is seen to produce a precipitous decrease in the capillary pressure. This fall in pressure is associated with a decrease in the tissue pressure which, in this case, continues to decrease until the terminal arteriole begins to dilate. The flow through the arteriole is similarly reduced by the contraction. A significant point to note is the relationship between this flow (i.e., the capillary inflow) and the outflow of the capillary. When the terminal arteriole is dilated, the capillary outflow is less than the inflow by an amount equal to the net filtration flow. When the arteriole contracts, both flows decrease, but the capillary outflow is larger than the terminal arteriole flow. This is due to the increase in fluid re-absorption (with respect to filtration) associated with the decrease in intravascular pressure. Thus, one clear consequence of the arteriole (or pre capillary sphincter) vasomotion, is to produce quite a dynamic mode of capillary filtration and re-absorption.

To investigate the relative significance of the capillary

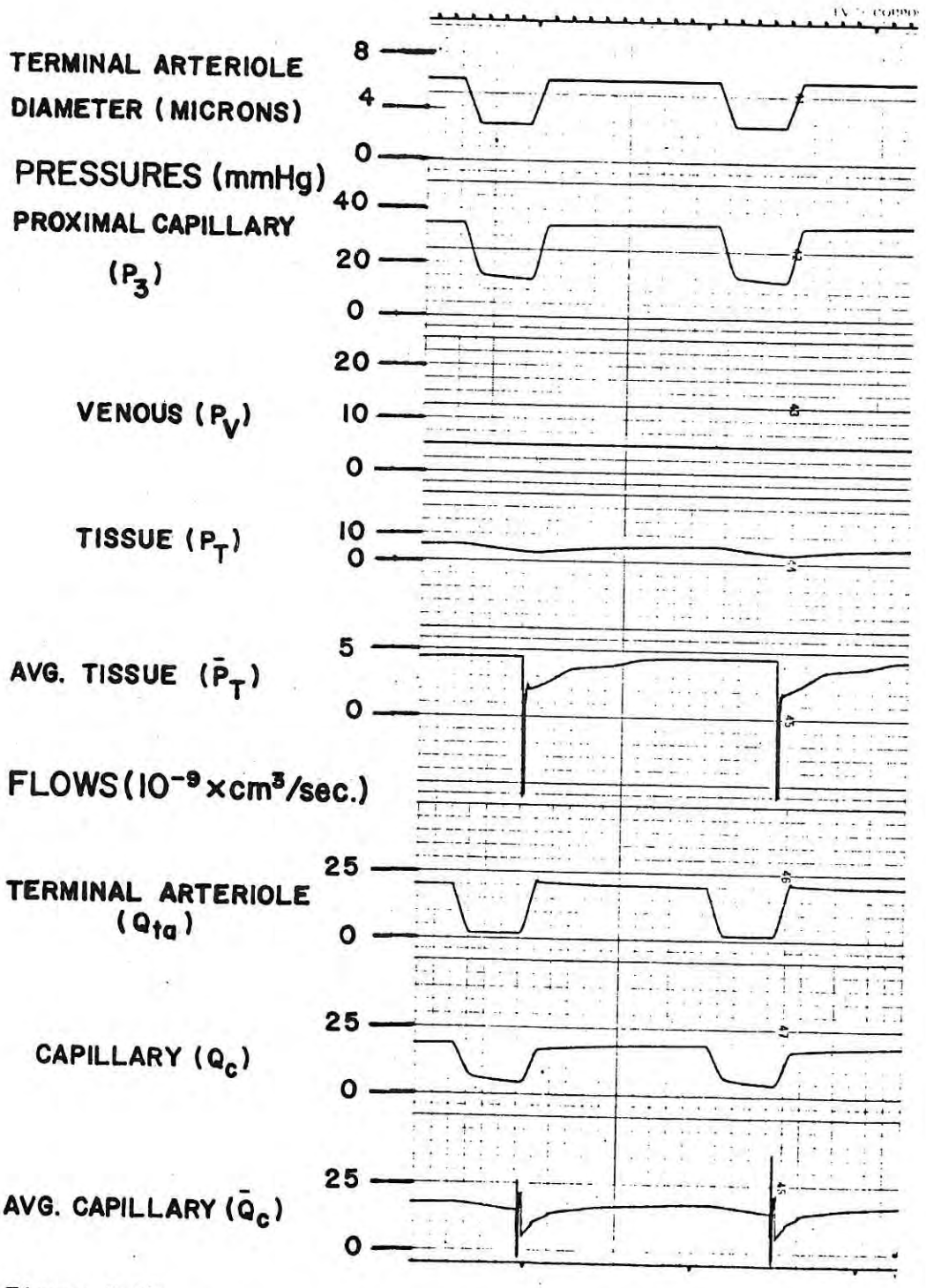

Figure 5.17.
HEMODYNAMICS ASSOCIATED WITH TERMINAL ARTERIOLE VASOMOTION. QUANTITIES SHOWN ARE THOSE CORRESPONDING TO THE MICRO-VASCULAR MODEL. TOP TIME MARKS ONE SECOND INTERVALS.

parameters on hemodynamics and capillary filtration, the mean tissue pressure and mean capillary outflow are measured for several different values of arterial and collecting venous pressure as these parameters are varied. For each value of venous pressure, the effect of the osmotic gradient's sensitivity to changes in tissue pressure is obtained by varying the value of $K_{\pi}C_T$ in the simulation. These results are shown in Table 5.3. The effect of the reference osmotic gradient is shown in Table 5.4

From these results summarized in these tables, it may be concluded that the significance of these capillary parameters as they relate directly to capillary flow is negligibly small. However, as expected, there is a strong dependency of the tissue pressure on both parameters at a given collecting venous pressure. In figure 5.18, the mean tissue pressure is plotted against venous pressure for three different values of $\Delta\pi_o$. Note that for $\Delta\pi_o = 20$, there is a considerable range of increase in venous pressure for which there is a rather small increase in tissue pressure.

This represents an effective buffering mechanism against elevations in venous pressure which is consistent with the experimental data summarized by Wiederhielm (1968) and Guyton (1971). Further, using the commonly accepted "normal" value of plasma osmotic pressure (25 mm Hg) and an effective osmotic pressure difference of approximately 20 mm Hg yields a tissue osmotic pressure of five mm Hg. Wiederhielm has indicated (1968) that the average protein concentration in the interstitial space may be as high as 2-3%, corresponding to

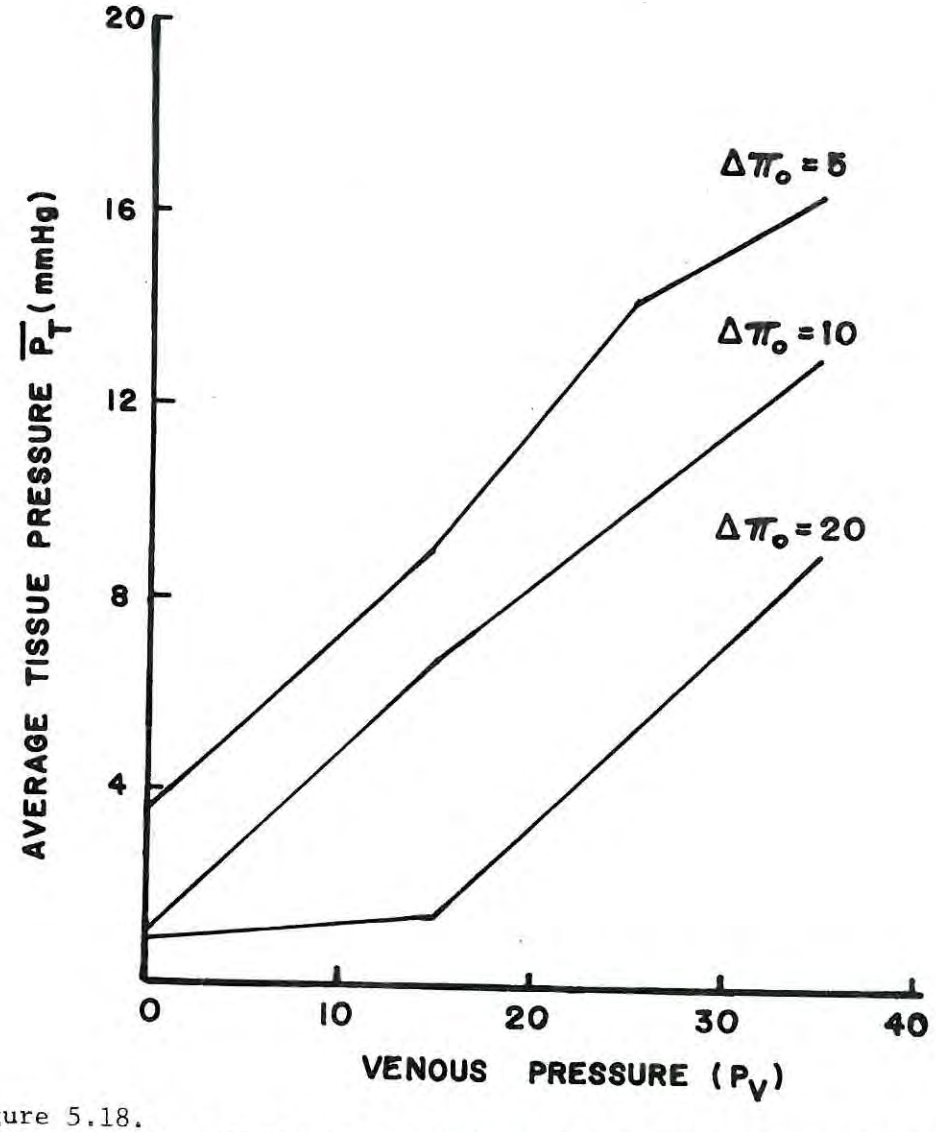

Figure 5.18.
TISSUE FLUID PRESSURE DEPENDENCE ON VENOUS PRESSURE. $\Delta\pi_o$ IS THE REFERENCE OSMOTIC PRESSURE DIFFERENCE (CAPILLARY - TISSUE)

Table 5.3. Mean tissue pressure P_T and capillary outflow $\bar{Q}_v$ for different values of central venous pressure P_V as a function of $K_\pi C_T$. Pressures in units of mm Hg, flows in units of 10^{-9} $cm^3 sec^{-1}$.

	$P_V = 0$		$P_V = 15$		$P_V = 35$	
$K_\pi C_T$	$\bar{P}_t$	$\bar{Q}_v$	$\bar{P}_t$	$\bar{Q}_v$	$\bar{P}_t$	$\bar{Q}_v$
0	2.9	19	12.8	13	22	4.8
1	1.0	19	6.8	13	13	5.3
3	.7	19	3.2	13	7	5.3

Table 5.4. Mean tissue pressure $\bar{P}_T$ and capillary outflow $\bar{Q}_v$ for different values of central venous pressure P_V as a function of reference osmotic gradient. Pressures in units of mm Hg, flows in units of 10^{-9} $cm^3 sec^{-1}$. Data are for $K_\pi C_T = 1$.

	$P_V = 0$		$P_V = 15$		$P_V = 35$	
$\Delta\pi_o$	$\bar{P}_t$	$\bar{Q}_v$	$\bar{P}_t$	$\bar{Q}_v$	$\bar{P}_t$	$\bar{Q}_v$
5	4.0	12.5	9.0	13	16.5	5
10	1.0	19.0	6.8	13	13	5
20	.9	19	1.5	11.8	9	5.4

a colloid osmotic pressure of about 5-8 mm Hg. It would thus appear that the values of the parameters used and the dynamics observed indeed reflect the physiological evidence.

ii. Controlled Vasomotion

Controlled vasomotion is the process whereby the terminal arteriole diameter is adjusted in accordance with the local tissue needs. The simulation of this process (see Chapter Four, Section IV-D for details) results in a dynamic system which is quite different in several characteristics from the uncontrolled case. In the controlled case, the terminal arteriole diameter is sensitive to tissue pressure, and as such, is dependent on all factors which affect tissue pressure.

In order to investigate the sensitivity and dynamics of the basic control process, the upper and lower tissue pressure activation thresholds (eq. 4.22) are varied and the resultant dynamics recorded. In Table 5.5, the results of one such sequence are shown. The upper and lower thresholds correspond to the values of instantaneous tissue pressure which will precipitate contraction and dilation of the terminal arteriole. The quantity T_t is the total period of the resultant dynamics, and T_c is the portion of this time that the vessel is contracted. The quantity (Q_r) is the ratio of the actual capillary flow to the maximum steady state capillary flow (i.e., that which would occur if the vessel maintained its maximum dilated diameter).

From Table 5.5, it is seen that for each threshold pair, there is a corresponding mean tissue pressure which is obtained.

Table 5.5... Effect of varying threshold levels on mean tissue pressure ($\overline{P}_T$), vasomotion period (T_t), contraction time (T_c) and flow ratio (Q_r). See text for definitions. Pressures in units of mm Hg, time in seconds. Data are for $\Delta\pi_o = 25$.

Tissue Pressure Thresholds						
Upper	Lower	P_T	T_t	T_c	T_c/T_t	Q_r
0	-4	-2	10.4	5.9	.77	.602
1	-4	-1.4	14.2	7.4	.52	.641
2	-4	-0.4	20.4	6.7	.32	.735
2.3	-4	+0.4	26.4	6.9	.26	.80
2.3	+1	+1.6	18.0	1.5	.08	.96

Table 5.6... Effect of varying threshold levels on mean tissue pressure ($\overline{P}_T$), vasomotion period (T_t), contraction time (T_c) and flow ratio (Q_r). See text for definitions. Pressures in units of mm Hg, time in seconds. Data are for $\Delta\pi_o = 10$.

Tissue Pressure Thresholds						
Upper	Lower	$\overline{P}_T$	T_t	T_c	T_c/T_t	Q_r
+2.3	+1.0	+1.8	11.8	9.7	.82	.217
+4	+1.0	+2.4	15.2	11.7	.78	.304
+5	+2.0	+3.5	11.4	7.1	.62	.450
+7.5	+6.0	+1.3	13.2	2.2	.17	.910

The value of this mean lies between the threshold values, and is determined by the dynamics in a rather complex way. Thus, with increasing mean tissue pressure, the vasomotion period may increase or decrease. However, there is a consistent decrease in the ratio of contraction time to total period. This requires that the absolute contraction time itself behave in accordance with the prevailing period for a given tissue pressure level. The result of this decreasing ratio is producing higher levels of flow associated with increasing mean tissue pressure.

It should be emphasized, however, that it is incorrect to associate a certain tissue pressure with a certain flow fraction. It is clearly possible to obtain the same average tissue pressure for two different values of osmotic pressure difference (i.e., either changed plasma levels or tissue levels). In this case, the control dynamics would maintain the proper tissue parameters, but, in so doing, the state of the vascular diameter and associated hemodynamics would not be the same. To illustrate this, in Table 5.6 are listed data similar to that of Table 5.5 but for an osmotic reference pressure difference of 10 mm Hg. This would correspond to a reduction in normal plasma level or an elevation in the tissue level. It is noted from Table 5.6 that though the flow ratio Q_r increases with increasing tissue pressure, as was determined from Table 5.5, similar absolute values of tissue pressure (c.f. last row of Table 5.5 with first row of Table 5.6) give rise to quite different dynamics. Since it is our objective to further study the basic significance of this process and its

interaction with post capillary dynamics, threshold levels of +1 and +4 mm Hg are used for the lower and upper levels respectively for the remainder of the analysis. These values are consistent with mean values obtained in the bat wing (Wiederhielm, 1969).

In figure 5.19 the vasomotion period is shown as a function of the perfusion pressure at a constant venous pressure. The parametric effect of the osmotic pressure difference ($\Delta\pi_o$) is quite apparent and results in a generally lower period for the smaller value. Note also that the fundamental period is a double valued function of the perfusion pressure. This is a manifestation of the complex capillary interactions already described.

In figure 5.20 one aspect of the hemodynamic significance of the control process is illustrated and compared with experimental data. In the bottom part of the figure, the ratio of contraction duration to vasomotion period, as derived from the Model, is plotted as a function of perfusion pressure for venous pressures of five and ten mm Hg (short dashed and solid lines respectively). Superimposed (closed circles) are the data of Wiedeman (1966) obtained by observing the terminal arterial contraction duration in response to elevated arterial pressure. As can be seen, the experimental data fit very well the characteristics predicted by the Model.

In the upper part of the figure, the capillary flow which is associated with the vasomotion characteristics is illustrated. The value at 70 mm Hg, which is taken as the control perfusion pressure, is normalized to unity. The result indicates that the consequence

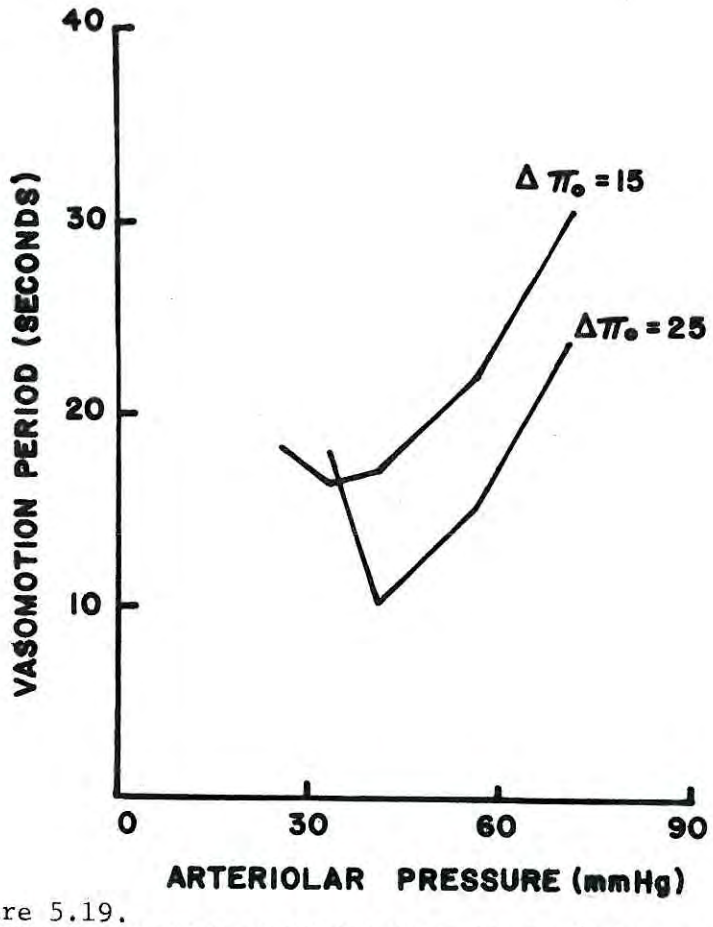

Figure 5.19.
VASOMOTION PERIOD DEPENDENCE ON PRESSURE
$\Delta\pi_o$ IS REFERENCE OSMOTIC PRESSURE DIFFERENCE

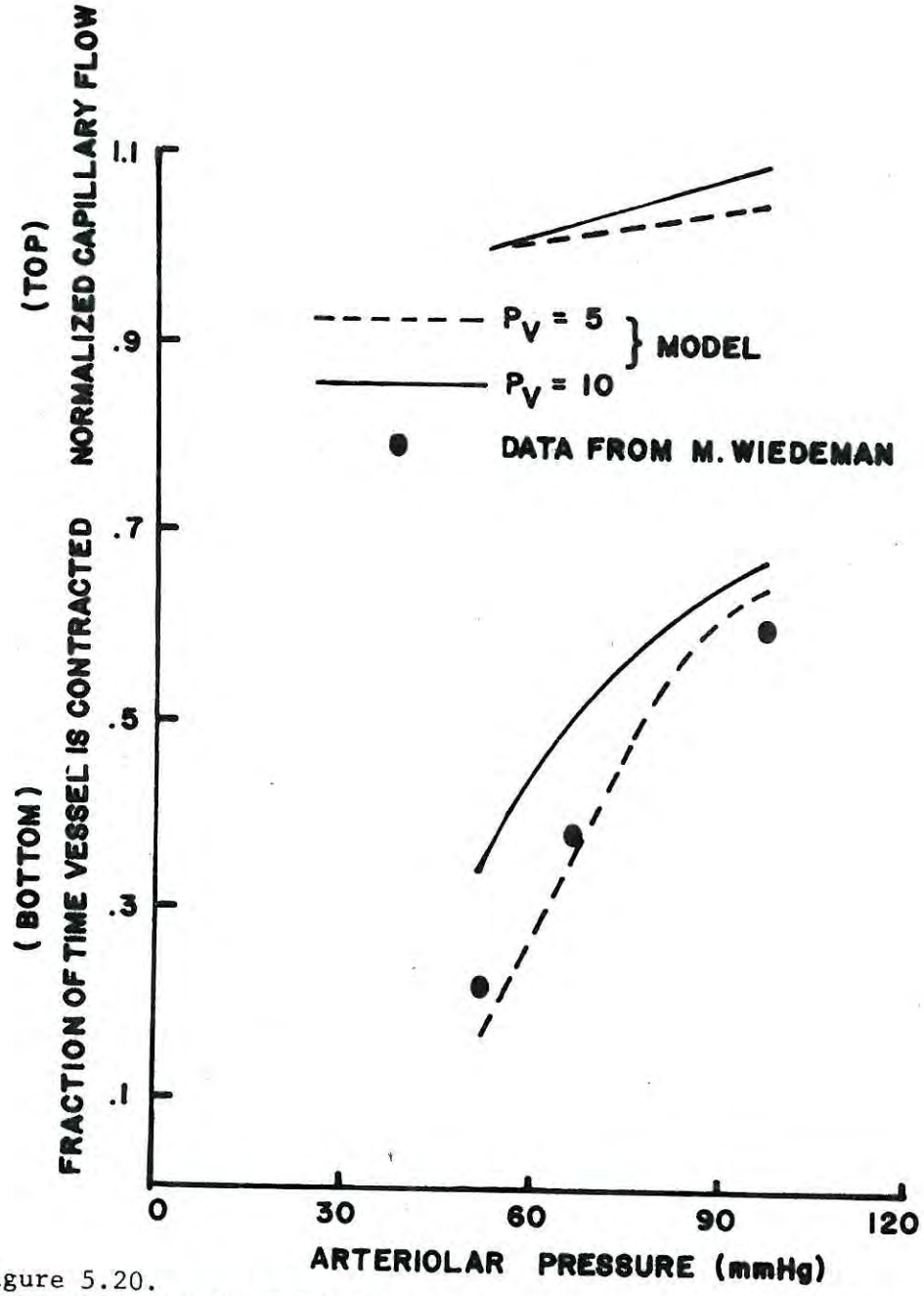

Figure 5.20.
CONTRACTION DURATION AND CAPILLARY FLOW DEPENDENCE ON ARTERIOLAR PRESSURE

of the vasomotion dynamics is an effective capillary flow autoregulation.

4. Effect of Venomotion and Vasomotion on Capillary Flow

In figure 5.21 the combined effect of venomotion and terminal arterial and pre capillary sphincter vasomotion on capillary flow is illustrated. The results shown are for uniform contraction at three different venomotion frequencies. The large rise in capillary flow which is noted is associated with the dilation phase of vasomotion (sphincter opening). Superimposed on this flow change is a smaller and higher frequency fluctuation, due to venomotion. For each of the venomotion frequencies shown, the capillary flow component due to venomotion is larger when the sphincters are fully open. Thus, for example, at a venomotion frequency of .5 Hz (e), the peak to peak capillary flow modulation produced by venomotion is 4×10^{-9} cm^3sec^{-1} when the sphincter is open, and 2.5×10^{-9} cm^3sec^{-1} when the sphincter is at its minimum diameter. However, when the venomotion contribution is expressed as a percent of the maximum flow, we find that when the sphincter is in its contracted state the modulation in capillary flow due to venomotion is 50%.

From these results, then, it would appear that under normal conditions and when the sphincters are fully dilated the capillary flow is mainly determined by pre capillary dynamics. With decreasing terminal arteriole diameter, the modulation in capillary flow is determined principally by post capillary dynamics.

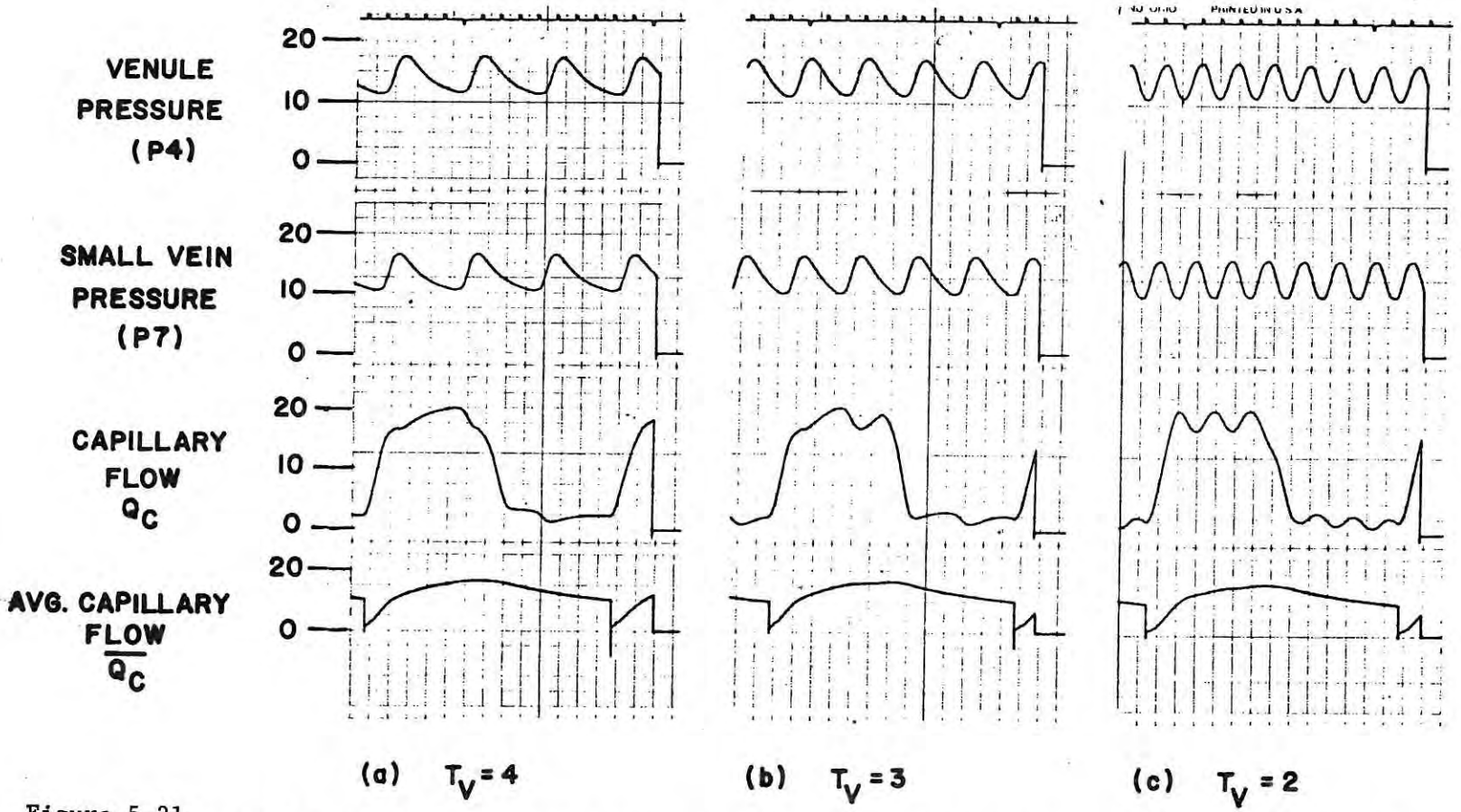

Figure 5.21.
COMBINED EFFECT OF VENOMOTION AND VASOMOTION ON CAPILLARY FLOW. T_V IS FUNDEMENTAL PERIOD OF VENOMOTION IN SECONDS, PRESSURES IN mmHg, FLOWS IN UNITS OF $10^{-9} cm^3/sec$, TIME MARKS AT ONE SECOND INTERVALS